

MODELLING, ESTIMATION AND PATH LENGTH CONTROL OF RING LASER GYROSCOPE

A PROJECT REPORT

submitted by

SUHAIB J.

(Reg. No. TKM21EEII10)

to

the APJ Abdul Kalam Technological University
in partial fulfillment of the requirements for the award of the Degree

of

Master of Technology

in

Electrical and Electronics Engineering

with specialisation in

Industrial Instrumentation and Control



Department of Electrical and Electronics Engineering

TKM College of Engineering Kollam

Kollam - 691 005

JUNE 2023

DECLARATION

I undersigned hereby declare that the project report entitled "**Modelling, estimation and path length control of Ring Laser Gyroscope**", submitted for partial fulfilment of the requirements for the award of the degree of Master of Technology in Electrical and Electronics Engineering with specialisation in Industrial Instrumentation and Control, of the APJ Abdul Kalam Technological University, Kerala is a bonafide work done by me under the supervision of *Dr. Mathew P Abraham*, Project Internal Supervisor, Assistant Professor, Department of Electrical and Electronics Engineering, *Mrs. Nisha. S. Dathan*, Project External Supervisor, Scientist Engineer 'SF', ISRO Inertial Systems Unit, Thiruvananthapuram, *Prof. Amal A.*, Project Co-ordinator, Assistant Professor, Department of Electrical and Electronics Engineering, and *Prof. Sumayya Jaleel*, Assistant Professor, Department of Electrical and Electronics Engineering. This submission represents my ideas in my own words and where ideas or words of others have been included. I have adequately and accurately cited and referenced the original sources. I also declare that I have adhered to ethics of academic honesty and integrity and have not misrepresented or fabricated any data or idea or fact or source in my submission. I understand that any violation of the above will be a cause for disciplinary action by the institute and/or the University and can also evoke penal action from the sources which have thus not been properly cited or from whom proper permission has not been obtained. This report has not been previously formed the basis for the award of any degree, diploma or similar title of any other University.

Kollam
June 26, 2023

SUHAIB J.

DEPARTMENT OF ELECTRICAL AND ELECTRONICS ENGINEERING

TKM COLLEGE OF ENGINEERING KOLLAM-691 005



CERTIFICATE

This is to certify that the project report entitled " **Modelling, estimation and path length control of Ring Laser Gyroscope** " submitted by **SUHAIB J. , (Reg. No. TKM21EEII10)** of fourth semester to the APJ Abdul Kalam Technological University in partial fulfillment of the requirements for the award of the Degree of Master of Technology in Electrical and Electronics Engineering with specialisation in Industrial Instrumentation and Control, is a bonafide record of the Project done by him under our guidance and supervision. This report in any form has not been submitted to any other University or Institute for any purpose.

Dr. Mathew P. Abraham

Internal Project Supervisor
Assistant Professor
Department of Electrical & Electronics Engg
TKM College of Engineering Kollam

Mrs. Nisha. S. Dathan

External Project Supervisor
Sci/Engr. 'SF'
DDH, OELGD, ISG, AIS
ISRO Inertial Systems Unit Thiruvananthapuram

Prof. Shanavas T. N

Associate Professor and PG Co-ordinator
Department of Electrical & Electronics Engg
TKM College of Engineering Kollam

Dr. Sabeena Beevi. K

Associate Professor and Head
Department of Electrical & Electronics Engg
TKM College of Engineering Kollam

ACKNOWLEDGEMENT

A lot of effort and hard work has been put into this project in course of its presentation. However, it would not have been possible without the kind support and help of many individuals and other sources. I would like to extend my sincere thanks to all of them. I take this opportunity to express my deep sense of gratitude and sincere thanks to all who helped me to complete this project report successfully.

I thank God Almighty for paving my way throughout the project. I thank *Dr. Sabeena Beevi. K*, Associate Professor and Head, Department of Electrical and Electronics Engineering and *Prof. Shanavas T. N*, PG Co-ordinator, Department of Electrical and Electronics Engineering for their support and help. I express my sincere thanks to *Dr. Imthias Ahamed T P.*, Head of Centre for Artificial Intelligence, for his valuable help.

I am greatly thankful to my internal project supervisor *Dr. Mathew P. Abraham*, Assistant Professor, Department of Electrical and Electronics Engineering, for his supervision, and helpful suggestions. I would like to express my special gratitude to my external project supervisor *Mrs. Nisha. S. Dathan*, Scientist Engineer 'SF', ISRO Inertial Systems Unit, Thiruvananthapuram, for her valuable guidance, supervision and support throughout the project. I want to acknowledge the contributions and support of *Mrs. Jyothi Janardanan*, Scientist Engineer 'SF', ISRO Inertial Systems Unit, Thiruvananthapuram. I am expressing my sincere thanks to *Prof. Amal. A*, Project Co-ordinator, Assistant Professor, Department of Electrical and Electronics Engineering, and *Prof. Sumayya Jaleel*, Assistant Professor, Department of Electrical and Electronics Engineering, for the positive criticism and valuable comments.

Finally, I thank my parents and friends who directly and indirectly contributed to the successful completion of my project.

SUHAIB J.

ABSTRACT

A gyroscope is a form of measurement equipment that relies on the principle of momentum conservation, stating that a rotating object will continue to rotate unless acted upon by an external force. This project focuses on a specific type of gyroscope called a ring laser gyroscope, which utilizes the Sagnac effect. The ring laser gyroscope is susceptible to various disturbances, such as fluctuations in ambient temperature. These disturbances can lead to significant deviations between the output data and the actual values, resulting in inaccurate angular measurements.

One of the factors affected by temperature change in the ring laser gyroscope is the path length. The path length refers to the total distance travelled by the counter-propagating light beams, which generates the interference pattern used to determine the angular rate. The laser gain profile should operate within the peak region for accurate angular rate measurements. However, the self-heating caused by temperature changes significantly alters the path length, shifting the operating point away from the peak and into one of the off-peak regions. To address this issue, adjustments can be made to the path length by modifying the refractive index of the air column and employing operating mode switching. These adjustments aim to bring the system back to its peak operating point. However, the current control system requires further refinement to achieve precise control, as it gets subjected to self-heating and external temperature changes. This research proposes a control strategy named model reference adaptive control, which treats the path length loop as a system and introduces external corrections by referencing a desired model system. By utilizing this approach, the system is concluded that the system will perform more effectively despite temperature fluctuations, leading to improved outcomes.

Contents

ABSTRACT

List of Tables	i
-----------------------	----------

List of Figures	ii
------------------------	-----------

ABBREVIATIONS	v
----------------------	----------

NOTATIONS	vi
------------------	-----------

1 INTRODUCTION	1
-----------------------	----------

1.1 GENERAL BACKGROUND OF GYROSCOPES	1
--	---

1.2 OBJECTIVES	7
--------------------------	---

1.3 SCOPE	8
---------------------	---

1.4 ORGANISATION OF REPORT	8
--------------------------------------	---

2 LITERATURE REVIEW	10
----------------------------	-----------

2.1 OVERVIEW	10
------------------------	----

2.2 STUDY OF RING LASER GYROSCOPES	11
--	----

2.2.1 Fundamentals of the Ring Laser Gyro	11
---	----

2.2.2 The Ring Laser Gyro	11
-------------------------------------	----

2.2.3 Laser Gyros with Total reflection prisms.	11
---	----

2.3 WORKS ON PATH LENGTH CONTROL FOR RING LASER GYROSCOPES	12
--	----

2.3.1 Development of control algorithm for Ring Laser Gyroscope	12
---	----

2.3.2 Implementation of control algorithm for Ring Laser Gyroscope	13
--	----

2.4 WORKS ON OUTPUT NOISE FILTERING AND COMPENSATION FOR RING LASER GYROSCOPES	13
---	----

2.4.1	Application of the Wavelet packet analysis in the RLG strapdown inertial navigation system	13
2.4.2	Laser gyro temperature compensation using modified RBFNN	14
2.4.3	Temperature drift modelling and compensation of RLG based on PSO tuning SVM	14
2.4.4	Adaptive H_{∞} Kalman filter-based random drift modelling and compensation method for ring laser gyroscope	15
2.5	SUMMARY	15
3	METHODOLOGY	16
3.1	OVERVIEW	16
3.2	PATH LENGTH CONTROL LOOP STUDIES	16
3.2.1	Path length control loop	16
3.2.2	Modelling of the existing path length control loop	18
3.2.3	Thermal sensitivity modelling of path length control loop	22
3.3	CONTROL SYSTEM DESIGN	23
3.3.1	Model Reference Adaptive PID Control	23
3.4	SUMMARY	32
4	RESULTS	33
4.1	OVERVIEW	33
4.2	RESULTS	34
4.2.1	Frequency responses of path length control loop in open and closed loop conditions for various band pass filter gains	34
4.2.2	Mathematical models derived from frequency responses	42
4.2.3	Validation of mathematical model using Step response	42
4.2.4	Thermal sensitivity model	46
4.2.5	Outcomes of model reference adaptive control	47
4.2.6	SUMMARY	51
5	CONCLUSION	52
5.0.1	CONCLUSIONS	52
5.0.2	RECOMMENDATIONS	53

5.0.3 SCOPE FOR FURTHER WORK 53

REFERENCES

List of Tables

4.1	Stability margins from bode plots.	41
4.2	Mathematical models derived using control system toolbox.	42
4.3	Theoretical step response parameters.	45
4.4	Actual step response parameters.	45
4.5	Phase offset actual step response parameters.	45

List of Figures

1.1	Structure of a mechanical gyroscope.	1
1.2	Structure of a MEMS gyroscope.	2
1.3	Coriolis effect.	2
1.4	The Sagnac effect.	3
1.5	Ring Laser Gyroscope.	4
1.6	Laser gain profile.	5
3.1	Path length control loop.	17
3.2	Path length control element.	17
3.3	Open loop frequency response Block diagram.	19
3.4	Closed loop frequency response Block diagram.	20
3.5	System identification toolbox in Matlab.	21
3.6	Control system design toolbox in Matlab.	22
3.7	Thermal chamber for various temperature tests.	23
3.8	Adaptive control Block diagram.	24
3.9	Model Reference Adaptive control Block diagram.	25
3.10	Feedback Control system.	28
3.11	Model Reference Adaptive Control method.	30
3.12	Simulation block diagram of proposed model reference adaptive control.	32
4.1	Experimental frequency response plot of open loop system for bandpass filter gain 5.	34
4.2	Frequency response plot of open loop system for bandpass filter gain 5 generated with Matlab.	34

4.3	Experimental frequency response plot of open loop system for bandpass filter gain 10.	35
4.4	Frequency response plot of open loop system for bandpass filter gain 10 generated with Matlab.	35
4.5	Experimental frequency response plot of open loop system for bandpass filter gain 15.	36
4.6	Frequency response plot of open loop system for bandpass filter gain 15 generated with Matlab.	36
4.7	Frequency response plot of open loop system with PI controller in series, for bandpass filter gain 5.	37
4.8	Frequency response plot of open loop system with PI controller in series, for bandpass filter gain 10.	37
4.9	Frequency response plot of open loop system with PI controller in series, for bandpass filter gain 15.	38
4.10	Experimental frequency response plot of closed loop system for bandpass filter gain 5.	38
4.11	Frequency response plot of closed loop system for bandpass filter gain 5 generated with Matlab.	39
4.12	Experimental frequency response plot of closed loop system for bandpass filter gain 10.	39
4.13	Frequency response plot of closed loop system for bandpass filter gain 10 generated with Matlab.	40
4.14	Experimental frequency response plot of closed loop system for bandpass filter gain 15.	40
4.15	Frequency response plot of closed loop system for bandpass filter gain 15 generated with Matlab.	41
4.16	Experimental step response.	43
4.17	Step response generated from Matlab using theoretical model for bandpass filter gain 5	43
4.18	Step response generated from Matlab using theoretical model for bandpass filter gain 10	44

4.19	Step response generated from matlab using theoretical model for bandpass filter gain 15	44
4.20	Bode plot of the thermal sensitive model developed using Matlab.	46
4.21	Step response of uncontrolled plant compared with the response of reference model.	47
4.22	Step response of controlled plant compared with the response of reference model.	48
4.23	Comparison of responses before and after model reference adaptive control. . .	48
4.24	Sinusoidal response by the reference model and plant model without adaptive control.	49
4.25	Sinusoidal response by the reference model and plant model with model reference adaptive control.	49
4.26	Comparison of sine responses of plant and reference with and without model reference adaptive control.	50
4.27	Variation happening in the values of θ_1 and θ_2 with respect to time for step input.	50

ABBREVIATIONS

ARMA	Auto Regressive Moving Average
CL	Closed Loop
FLP	Forward Linear Prediction
FPGA	Field Programmable Gate Array
FRA	Frequency Response Analyzer
HFO	High Frequency Oscillator
LABVIEW	Laboratory Virtual Instrument Engineering Workbench
MATLAB	Matrix Laboratory
MEMS	Micro Electro Mechanical System
MIMO	Multiple Input Multiple Output
MIT	Massachusetts Institute of Technology
MRAC	Model Reference Adaptive Control
ODE	Ordinary Differential Equation
OL	Open Loop
PI	Proportional Integral
PID	Proportional Integral Derivative
PSO	Particle Swarm Optimisation
RBF	Radial Basis Function
RBFNN	Radial Basis Function Neural Network
RLG	Ring Laser Gyroscope
RLS	Recursive Least Squares
SISO	Single Input Single Output
TRPLG	Total Reflection Prism Laser Gyroscope

NOTATIONS

A Area, cm^2

L Length, cm

F Frequency, Hz

Ω Angular Rate, $^\circ/Hz$

Chapter 1

INTRODUCTION

1.1 GENERAL BACKGROUND OF GYROSCOPES

Gyroscopes are utilized to measure an object's angular velocity. Conventional gyroscope consist of a freely rotating spinning disc, capable of orienting itself in any direction. The functioning of a gyroscope is based on the principle of momentum conservation, which dictates that a spinning body will continue spinning unless acted upon by an external force. There are various types of gyroscopes, each operating on different principles. One such type is the mechanical gyroscope, which relies on momentum conservation.

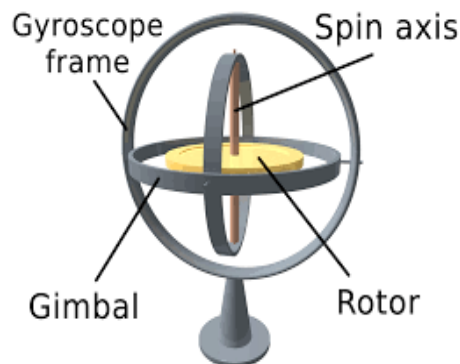


Figure 1.1: Structure of a mechanical gyroscope.

It comprises a spinning disc with a specific mass, rotating freely within gimbals-structures that support the disc and allow it to rotate on its axis. While the gimbals can move in any direction, they cannot alter the spinning motion of the disc. In essence, a gyroscope can be likened to a top attached with gimbals. Interestingly, similar tops were commonly used in ancient Greece, Rome, and China. In 1973, John Serson developed a device akin to a gyroscope for locating

the horizon in foggy conditions. Another significant contribution was made by scientist Leon Foucault, who conducted a gyroscope experiment based on Earth's rotation. When subjected to external torques along a specific axis, a gyroscope's orientation can be measured through a phenomenon known as precession. Precession occurs when a rotating object is influenced by an external torque perpendicular to its rotational axis. By detecting this rotation about the spin axis, information can be transmitted to a drive or another device, which applies torque in the opposite direction, effectively reversing the precession and maintaining the orientation. Alternatively, precession can be prevented by utilizing two gyroscopes oriented perpendicularly to each other.

The next category of gyroscopes are the microelectromechanical system gyroscopes known as the MEMS gyroscopes, which work under the effect of Coriolis force[1]. MEMS gyroscopes

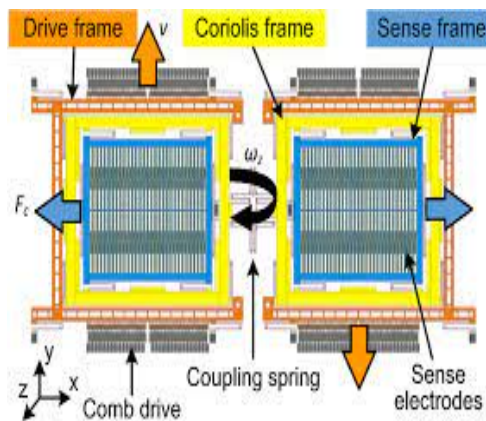


Figure 1.2: Structure of a MEMS gyroscope.

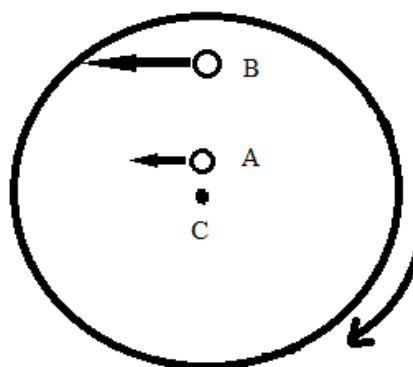


Figure 1.3: Coriolis effect.

commonly utilize a vibrating mechanical device as a sensor element to measure angular velocity. The Coriolis effect, a transient phenomenon, can be observed in various situations. Let's

consider two individuals, A and B, positioned on a rotating platform. Their velocities relative to the floor will differ, with those farther from the centre moving at higher speeds while those closer to the middle moving at comparatively slower rates. As one moves from the centre towards the periphery, the speed gradually increases due to the Coriolis effect, which refers to the increment in tangential speed caused by radial velocity. MEMS gyroscopes offer a more economical alternative to other gyroscopes, employing embedded circuits and providing either analogue or digital output. These gyroscopes can incorporate multiple axes within a single component, enabling output with numerous degrees of freedom.

An additional classification pertains to Laser Gyroscopes, which operate based on the principle of the Sagnac effect. The Sagnac effect refers to the alteration in the distance travelled by light beams originating from a common source and reaching the same destination when exposed to a modification in the direction of their travel path.

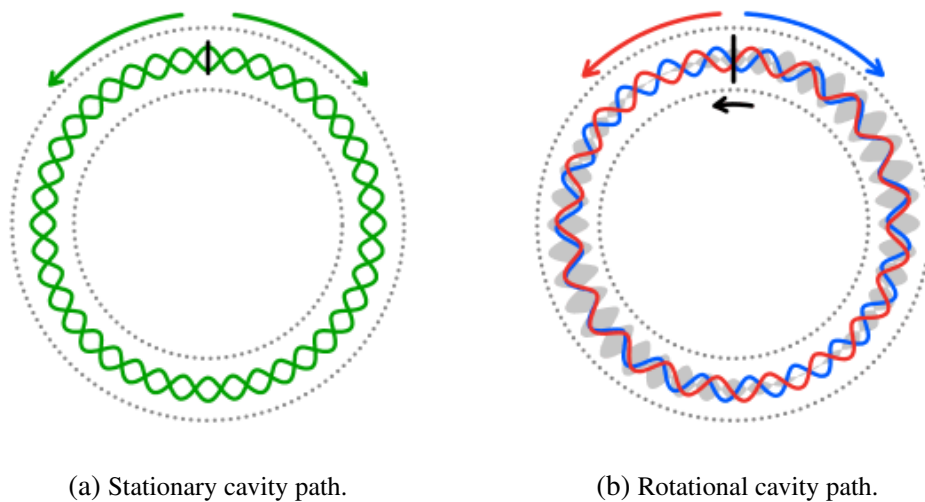
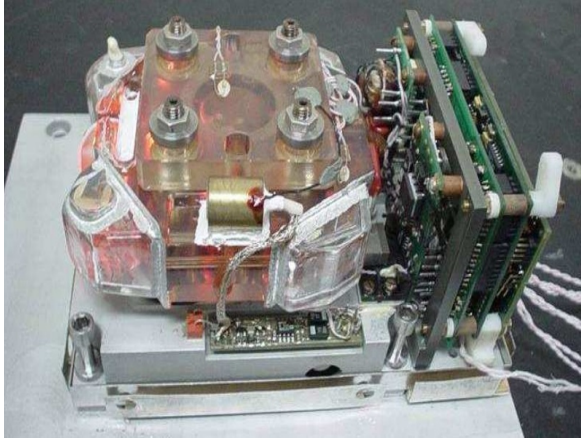
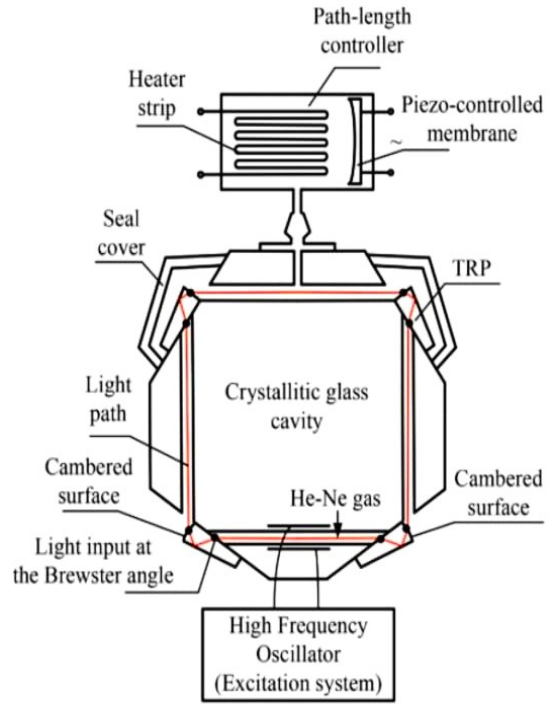


Figure 1.4: The Sagnac effect.

Total Reflection Prism Laser Gyroscopes (TRPLG) are gyroscopes that utilize a Total Reflection Prism to reflect light beams. The orientation change experienced by the TRPLG is influenced by the Sagnac effect. Consequently, counter-propagating beams converge at the target, leading to the production of interference patterns. Optical gyroscopes have been widely employed in strap-down aeroplanes' inertial navigators. The advancement of laser technology has rendered the need for gimbals obsolete, as rotation sensing can now be achieved within the laser's frame. The unique characteristic of lasers lies in their emission of coherent light, distinguishing them from other light sources. Optical cavities constitute a significant component of lasers, allowing the creation of standing waves through the reflection of light in various



(a) Total Reflection Prism laser Gyroscope(TRPLG).



(b) Internal structure of TRPLG.

Figure 1.5: Ring Laser Gyroscope.

patterns. For a standing wave pattern to form, it is essential that the path length consists solely of integral multiples of the wavelength. ie.

$$L = n\lambda \quad (1.1)$$

where n is an integer. Laser gyroscopes have become increasingly popular as viable options due to their remarkable precision and affordability. These gyroscopes, specifically ring laser gyroscopes (RLG), employ ring cavities to accurately measure angular rotation. By utilizing two laser beams travelling in opposite directions within a closed pathway formed by reflective prisms, RLG systems achieve highly precise and accurate angular measurements. The functionality of ring laser gyroscopes relies on the properties of electromagnetic radiation, as they detect rotational motion by observing an actual frequency disparity between the opposing light beams traversing a confined path. Excitation sources are incorporated into the closed pathway of an RLG to generate the necessary laser beams. The frequency difference between the two laser beams due to the rotation of the path is represented by,

$$\Delta f = \frac{4A}{L\lambda} \Omega \quad (1.2)$$

$$scale\ factor = \frac{4A}{L\lambda} \quad (1.3)$$

where the L is the Cavity path length, A is the Area enclosed by Laser beam path, Δf is Frequency shift and Ω is the Angular rotation rate[2]. Controlling the length of the path becomes crucial when variations in ambient temperature impact the path's length, causing the laser's operating point to shift away from the peak of its gain profile.

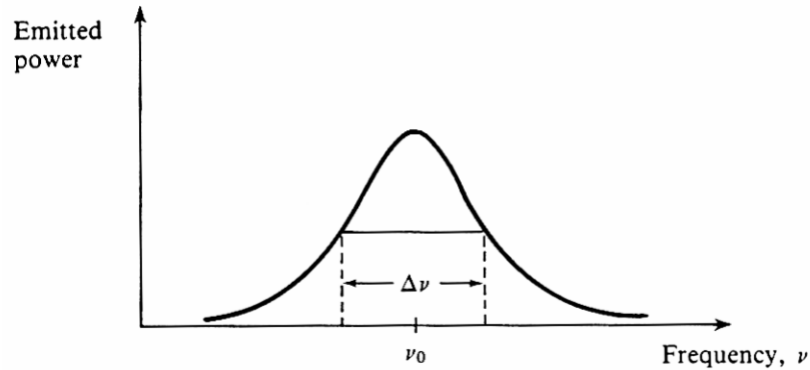


Figure 1.6: Laser gain profile.

RLG (Ring Laser Gyroscope) has a distinct advantage over conventional spinning gyroscopes due to the absence of moving parts, resulting in a frictionless system. Laser gyroscopes are widely used in navigation systems of commercial ships, aircraft, and even spacecraft. The advantages of using RLG are as follows,

- High Accuracy.
- Bias stability
- Wide dynamic range and high bandwidth.
- High scale factor stability.
- Low scale factor nonlinearity.

Control loops in Ring Laser Gyroscope

In laser gyroscopes, a **High-frequency oscillator** (HFO) loop is a feedback loop that helps maintain the laser intensity. Laser gyroscopes depend on the interference of laser beams to measure rotational motion accurately. The HFO loop in a laser gyroscope typically consists of the following components,

1. High-Frequency Oscillator: The high-frequency oscillator generates a stable and precise oscillating signal, typically in the megahertz or gigahertz range.

2. Intensity Detector: The envelope detector compares the interference pattern's intensity with required intensity setpoint.
3. Feedback Loop: The feedback loop adjusts the high-frequency oscillator's supply to sustain lasing at an optimal operating point. This helps keep the gyroscope laser source stable.

In a ring laser gyroscope (RLG), a **Dither loop** refers to a feedback control mechanism used to introduce and maintain a sinusoidal rate in the laser beams circulating within the gyroscope's ring cavity. The primary purpose of dithering in a ring laser gyroscope is to enhance the gyroscopic performance by improving measurement accuracy and stability. The dither loop typically operates by employing a phase-sensitive detection scheme. Dither loop works in a ring laser gyroscope as below,

1. Dither actuation: A required dither signal is introduced to the laser beams circulating within the ring cavity. This modulation is typically achieved by applying a voltage to piezo actuated dither in turn actuates the optical block.
2. Dither detection: The modulated laser beams are split into two counter-propagating beams within the ring cavity. These beams interfere with each other, resulting in an interference pattern. By using photodetectors, the phase difference between the two counter-propagating beams can be measured in terms of magnitude and phase of quadrature signals.
3. Feedback control: The measured dither amplitude and frequency are compared with a reference. Any deviation from the reference indicates an error or motion. The error signal is then corrected based on this deviation.
4. Correction: The error signal is processed and amplified, and then fed back to the laser source or other control elements within the gyroscope. This feedback signal adjusts the dither modulation, compensating for any rotation-induced phase difference and maintaining the gyroscope's output.

By continuously modulating and adjusting the dither signal based on the measured feedback, the dither loop helps to minimize measurement errors caused by environmental factors, such as temperature changes, vibrations, and other disturbances. It improves the stability, linearity, and accuracy of the ring laser gyroscope's output.

Dithering in a ring laser gyroscope is a well-established technique used in modern navigation systems, inertial guidance systems, and other applications that require precise and reliable angular rate measurements.

A **Path length control loop** refers to a feedback control mechanism used to stabilize the optical path length of a light beam within an interferometer or other optical system. The primary purpose of a PLC loop is to maintain the phase coherence of the light beam and ensure accurate and reliable interferometric measurements. The PLC loop works as,

1. Reference signal generation: A reference signal is generated as a mechanism for obtaining desired optical path length. This reference signal is typically a stable, high-frequency electrical signal that drives the actuator.
2. Path length sensor: The path length sensor measures the actual optical path length of the light beam. The sensor can be a simple detector, a phase sensor, or another interferometric element that measures the phase difference between the reference and measured signals.
3. Signal processing: The measured path length signal is preprocessed and compared with the reference signal, and any deviation is detected. The difference between the reference and measured signals is then amplified and filtered to produce the error signal.
4. Feedback actuator: The error signal is used to drive a feedback actuator that adjusts the optical path length to match the reference signal. The actuator can be a piezoelectric transducer, a mechanism that can control the position of optical elements or optics-based features.

By continuously adjusting the optical path length based on the error signal, the PLC helps to stabilize the phase coherence of the light beam. This stabilization is critical for achieving accurate and reliable interferometric measurements, such as in interferometric distance sensing, gravitational wave detection, or other precision metrology applications.

1.2 OBJECTIVES

- Control loop studies of the existing control system for Path length.
- Developing a mathematical model of the path length control system that incorporates temperature variations to achieve a thermal-sensitive model.

- Designing an appropriate control strategy to maintain the operating point within the peak region of the laser gain profile by compensating for temperature variations in the working conditions, while also addressing any deficiencies in the existing path length control system.

1.3 SCOPE

Disturbances occurring in any process can significantly impact its output and overall performance. This holds true for inertial navigation systems, where gyroscopes play a crucial role in measuring angular position. Gyroscopes, particularly ring laser gyroscopes that operate based on the optical Sagnac principle, are susceptible to various disturbances arising from both the working environment and the system itself. One of the prominent challenges faced by ring laser gyroscopes is the impact of ambient temperature changes. Additionally, self-heating within the system poses another problem that affects gyroscope performance, which is the focal point of this project. Given that gyroscopes are extensively used for measuring the angular position of aircraft, it becomes imperative to rectify any potential errors to ensure accurate measurements. The safety of an aircraft relies heavily on its precise flight orientation. A critical metric in ring laser gyroscopes is scale factor stability, which plays a vital role in minimizing bias drift. In an ideal scenario, the normalized scale factor should be unity, although achieving this is challenging. Therefore, it is essential to control and maintain the scale factor close to unity to enable accurate angle rate measurement. As indicated in equation (1.3), the key to maintaining a constant scale factor lies in controlling the path length. Consequently, the methods discussed in this report regarding path length control and compensation hold significant importance in RLG use in real-time guidance and navigation systems.

1.4 ORGANISATION OF REPORT

The report is structured into 5 chapters. Chapter 1, Introduction, provides an overview of the project, outlining the general background, objectives, and organization of the report. Chapter 2 presents a comprehensive literature review on the project topic. Chapter 3, titled Methodology, focuses on developing a mathematical model of the system that accounts for the impact of var-

ious temperature effects and the control design. Chapter 4 presents the results of the study, and Chapter 5 provides the conclusion, summarizing the findings and discussing their implications.

Chapter 2

LITERATURE REVIEW

2.1 OVERVIEW

This chapter provides an overview of the notable research conducted on the analysis and control methods applied to path length control of laser gyroscopes, with a focus on enhancing the output accuracy. The primary objective of path length control is to mitigate disturbances and noise, thereby improving the correctness of the output. Various approaches have been explored in traditional path length control and gyroscope output filtration. In mirror-based laser gyroscopes, adjusting the mirrors that reflect the light beams is a common method for modifying the path length. By controlling the associated piezoelectric system, the mirror's position can be precisely adjusted, leading to a change in path length. Additionally, digital control systems and specialized structures have been developed for effective path length control. Wavelet analysis is another conventional method used for filtering out noise from desired output signals. It enables the analysis of signals in time-frequency space, allowing the extraction of desired signals while attenuating or eliminating unwanted noise. In the context of filtering gyroscope output from disturbance noises, Kalman filtering has been widely employed as a traditional method. However, advancements have led to the development of modified Kalman filtering techniques and machine learning-based systems as alternative approaches for improved filtering. This chapter discusses several path length control methods, output filtering techniques, and compensation methods that have been studied and developed to enhance the performance of laser gyroscopes.

2.2 STUDY OF RING LASER GYROSCOPES

2.2.1 Fundamentals of the Ring Laser Gyro

F. Aronowitz extensively explored the foundational principles underlying ring laser gyroscopes. The inception of ring laser gyroscopes dates back to 1962 when they were first put into operation. Over time, incremental advancements have been made to enhance their functionality and convenience. The operation of a ring laser gyroscope revolves around the Sagnac effect, which elucidates that the rotation of the cavity path results in a frequency alteration in two coherent beams of light travelling in opposite directions. This frequency change is directly proportional to the rotation of the cavity. In this particular work, the author provides a comprehensive explanation of the mathematical relationships between the frequency difference and the corresponding rotation of the cavity path. Furthermore, the author delves into the design structure of a ring laser gyroscope and offers a detailed discussion on the mathematical equations governing frequency and amplitude[2].

2.2.2 The Ring Laser Gyro

Authors Faucheux et al. provides a comprehensive review of the ring laser gyro (RLG), which is an extensively developed optical gyroscope based on the Sagnac phenomenon. In their article, they examine the advantages offered by RLG and explore various factors that can affect its performance. Specifically, they focus on two significant sources of error: gas fluxes in the active medium and the synchronization, or "locking," of counterpropagating waves. The authors pay special attention to the primary impact of mirror backscattering on the "locking" phenomenon and present solutions that have been devised to address this issue. Additionally, they identify several key design principles that should be considered during the construction of an RLG. The article offers valuable insights into the operation and optimization of RLG systems[3].

2.2.3 Laser Gyros with Total reflection prisms.

Y.V. Bakin et al. proposed the use of a total reflection prism in place of traditional reflecting mirrors in their work. The aim was to enhance the quality factor of the ring cavity and minimize backscattering, which is crucial for the advancement of laser gyroscope technology. To address this issue, the authors suggested incorporating a highly reflective surface to reflect inci-

dent light. Total reflection prisms were found to exhibit near-perfect reflectivity, making them a viable option for ring laser gyroscope technology development. The paper outlines a path length control scheme using heaters and describes the design structure of the reflection prism gyroscope. The total reflection prisms used in various applications included two, three, or four prisms. In the project, a ring laser gyroscope with four total reflective prisms was considered. The work offers valuable insights into the use of total reflection prisms and their potential in advancing laser gyroscope technology. Bakin et al. introduced a path length control scheme utilizing heaters and extensively elucidated the design structure of the reflection prism gyroscope in their study. Total reflection prisms were employed in a range of applications, typically consisting of two to four prisms. In this specific project, the ring laser gyroscope being investigated made use of four total reflection prisms. The authors' work offers comprehensive insights into the implementation and potential benefits of employing total reflection prisms in ring laser gyroscopes.

2.3 WORKS ON PATH LENGTH CONTROL FOR RING LASER GYROSCOPES

2.3.1 Development of control algorithm for Ring Laser Gyroscope

P. Shakira Begum et al. introduced a novel path length control approach that utilizes reflective mirrors and piezo drives controlled by an algorithm. A ring laser gyro requires stable laser beam intensity, a long cavity path, and an effective dithering mechanism to operate at peak performance. Hardware and control algorithm implementations are necessary for these three controls in RLGs. While most methods used to achieve these controls rely on linear algorithms, using non-linear algorithms based on the dynamics of the RLG can improve its performance. To this end, the authors conducted a study to investigate the basics of RLG control, simulated its dynamics to understand the non-linearities involved, and developed new control algorithms for regulating RLG performance. The study implemented these methods using MATLAB/Lab VIEW. The research provides valuable insights into the optimization of RLG control and highlights the potential of non-linear algorithms in improving RLG performance[4].

2.3.2 Implementation of control algorithm for Ring Laser Gyroscope

Prasanti. P et al. proposed a novel approach for controlling path length in ring laser gyroscopes (RLGs) using a path length control circuit developed with Lab VIEW and digital components. Path length, intensity, and dithering are critical factors that affect RLG performance. Variations in path length can lead to changes in intensity. By employing RLG model equations, the authors devised an algorithm to effectively manage path length, intensity, and dithering. They further implemented this algorithm in a field-programmable gate array (FPGA) by digitizing the output signals. The authors suggested that their technology holds potential for tracking, balancing, and regulating motion in fields such as robotics and spacecraft applications. The research offers a promising method for precise control and optimization of RLGs, with potential implications in various industries requiring accurate motion tracking and regulation[5].

2.4 WORKS ON OUTPUT NOISE FILTERING AND COMPENSATION FOR RING LASER GYROSCOPES

2.4.1 Application of the Wavelet packet analysis in the RLG strapdown inertial navigation system

G. Chuang et al. proposed the application of wavelet packet analysis as a method for filtering gyroscope data, aiming to enhance the precision and alignment of inertial navigation systems. Wavelet packet analysis involves the linear combination of wavelet functions. In this analysis, the signal is divided into a high-frequency signal and a low-frequency signal. Each of these signals is further decomposed recursively to ensure that the bandwidth of each component matches the overall spectrum bandwidth. By utilizing wavelet analysis, valuable signals are gathered in the low-frequency region, while noise signals are identified in the high-frequency region. The authors employed suitable software to simulate wavelet analysis and successfully demonstrated its effectiveness in rectifying errors that occurred in the output. This research showcases the potential of wavelet packet analysis as a valuable tool for signal filtering in gyroscopes, contributing to the improvement of inertial navigation system performance[6].

2.4.2 Laser gyro temperature compensation using modified RBFNN

In their study, J. C. Ding et al. proposed a method that combines the radial basis function neural network (RBFNN) with the Kohonen network and orthogonal least square algorithm. This combination offers several advantages, including improved classification capability of the Kohonen network, optimal selection of the orthogonal least square algorithm, enhanced compensation accuracy, and random selection of the RBFNN. The RBFNN is a three-layer forward neural network with multiple inputs and a single output. On the other hand, the Kohonen network is a neural network that classifies inputs by adjusting weights. In this method, the data is initially classified using the Kohonen network, and a hidden layer vector is formed. This vector is then used to train the RBFNN, which is modified and utilized to compensate for temperature changes in a ring laser gyroscope. The proposed approach demonstrates the effectiveness of combining these techniques to enhance the temperature compensation process in gyroscope systems[7].

2.4.3 Temperature drift modelling and compensation of RLG based on PSO tuning SVM

In their study, J. Cheng et al. address the challenges and limitations associated with least square methods and neural network-based compensations. To overcome these issues, they propose a novel method that utilizes particle swarm optimization (PSO) and tuning support vector machines (SVM). The method incorporates a forward-linear prediction filter (FLP) to ensure generalization. By employing the PSO algorithm, the parameters of the support vector machine can be efficiently tuned to achieve the desired prediction accuracy. Support vector machines are effective for data classification based on predefined boundaries, and a kernel function is employed to transform the data into higher dimensions when faced with complex classification scenarios. The Gaussian radial basis function (RBF) kernel is utilized as the kernel function in this particular method. The proposed approach offers a promising solution for accurate prediction and compensation by leveraging the benefits of PSO, SVM, and FLP in addressing the inaccuracies associated with existing methods[8].

2.4.4 Adaptive H_∞ Kalman filter-based random drift modelling and compensation method for ring laser gyroscope

Wang et al. conducted a study to investigate the impact of random drift on the output of ring laser gyroscopes (RLGs). They proposed a technique to simulate drift errors and correct inaccuracies in order to achieve precise measurements with RLGs. The conventional Kalman filter method for compensation was found to be unsuitable due to the requirement for a precise discrete state space model and knowledge of process and measurement noise properties. To address this issue, the authors suggested utilizing an error model known as the Auto Regressive Moving Average technique (ARMA). They further employed the H_∞ Kalman filter, an enhanced version of the Kalman filter, to estimate uncertainties. The random drift effect was analyzed using the Allan variance approach. The research provides insights into mitigating the impact of random drift in RLGs and presents a potential solution through the application of ARMA and the H_∞ Kalman filter.[9].

2.5 SUMMARY

In this chapter, we have explored various previous works related to path length control and output data filtering in ring laser gyroscopes, with a focus on mitigating the influence of disturbance effects. Different methods have been employed, ranging from traditional wavelet analysis to more recent machine learning approaches. Each method has its own strengths and limitations, leading researchers to continually modify and develop new techniques to enhance the performance of ring laser gyroscopes. It is important to note that the quality and advancement of these methods have not diminished over time; instead, they have improved through extensive research efforts. This continuous drive for improvement underscores the commitment of researchers in advancing the field of ring laser gyroscopes.

Chapter 3

METHODOLOGY

3.1 OVERVIEW

The main objectives of this project are to develop a model for the path length control system in a ring laser gyroscope and to implement appropriate corrections to the control strategy. The focus is on addressing the influence of ambient temperature changes on the path length and the resulting shift in the operating point of the laser from the peak of the laser gain profile. The methodology employed in this project involves temperature sensitivity modelling. A detailed procedure is followed to develop a model that captures the sensitivity of the gyroscope's path length to temperature variations. Once the modelling process is completed, a control strategy is formulated to effectively correct the path length loop based on temperature-induced changes. By successfully modelling the temperature sensitivity and implementing the correction strategy, the project aims to enhance the stability and accuracy of the ring laser gyroscope under varying ambient temperature conditions.

3.2 PATH LENGTH CONTROL LOOP STUDIES

3.2.1 Path length control loop

In order to maintain the path length of the coherent counterclockwise travelling beams in a ring laser gyroscope, a path length control loop is implemented. The desired path length should be an integral multiple of the wavelength to achieve a standing wave pattern. However, the path length-wavelength relationship can be affected by changes in ambient temperature. To adjust the

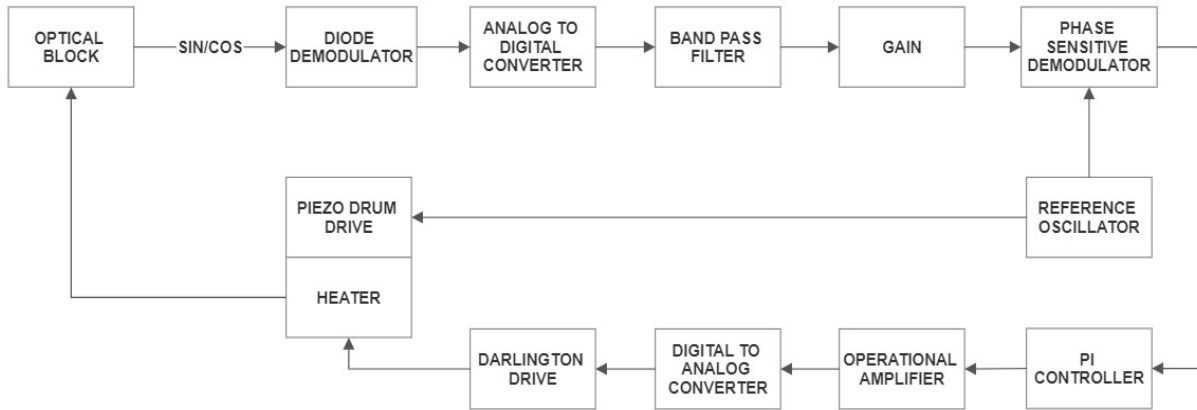


Figure 3.1: Path length control loop.

path length, the refractive index of the air column along the path is modified. This is achieved by changing the temperature of the air column. A proportional-integral (PI) controller is employed to control the temperature and thus regulate the refractive index. The PI controller takes into account the error between the desired path length and the actual path length and adjusts the temperature accordingly to maintain the desired path length. By continuously monitoring and adjusting the temperature of the air column through the PI controller, the path length control loop ensures that the path length remains at the desired multiple of the wavelength, compensating for any variations caused by ambient temperature changes. This control mechanism plays a crucial role in maintaining the stability and accuracy of the ring laser gyroscope.

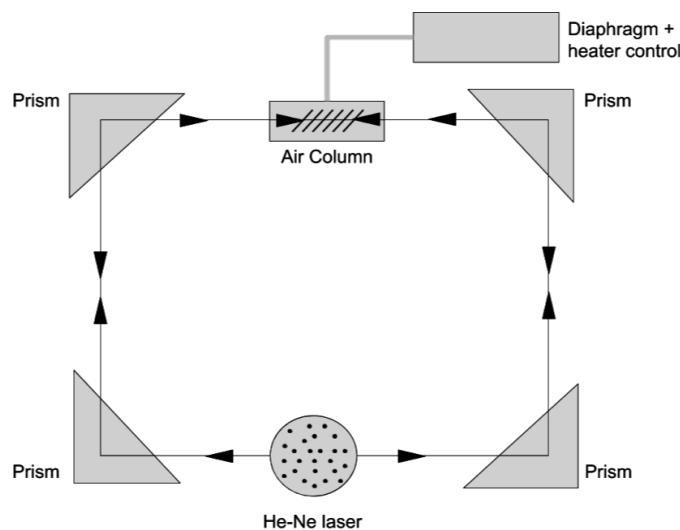


Figure 3.2: Path length control element.

The path length control system in the ring laser gyroscope incorporates a reference oscillator that generates a reference signal of a specific frequency. This reference signal is then

amplitude modulated to produce sinusoidal (sin) and cosine (cos) signals derived from the optical block. The sin and cos signals are fed to the piezo drum drive excitation associated with the heater block. After amplification, the modulated sin and cos signals are digitized and passed through a phase-sensitive demodulator. The demodulator multiplies the original reference signal with the modulated signal and calculates the phase difference between them. This phase difference, representing the path length error, is then used as input for a proportional-integral (PI) controller. The PI controller analyzes the phase change error from the demodulator and generates a control signal. This control signal is applied to the heater, causing the air column to be heated and thereby changing the refractive index. As a result, the path length is adjusted to the desired value. By continuously monitoring the phase difference and providing appropriate control signals to the heater, the PI controller ensures that the path length remains at the desired multiple of the wavelength, maintaining the stability and accuracy of the ring laser gyroscope.

3.2.2 Modelling of the existing path length control loop

To develop a model of the path length control loop, the sensor is tested in three different scenarios, each with a different bandpass filter gain. These scenarios allow for the evaluation of the system's behavior under various filter gain settings. The purpose of these tests is to gather data and observations that can be used to establish a mathematical representation of the path length control loop. During the testing, the sensor's response to input signals is recorded for each scenario. The input signals may include sine waves or other predetermined signals that are applied to the sensor. The response data is collected and analyzed to identify patterns and characteristics that can be used to develop the model. By comparing the sensor's response across the three scenarios with different bandpass filter gains, researchers can gain insights into how the filter gain affects the system's behavior. This information can be used to establish a mathematical model that accurately represents the dynamics of the path length control loop. The developed model will provide a valuable tool for understanding, analyzing, and optimizing the performance of the path length control loop in the ring laser gyroscope. It can also be used for further research, simulation, and control design purposes.

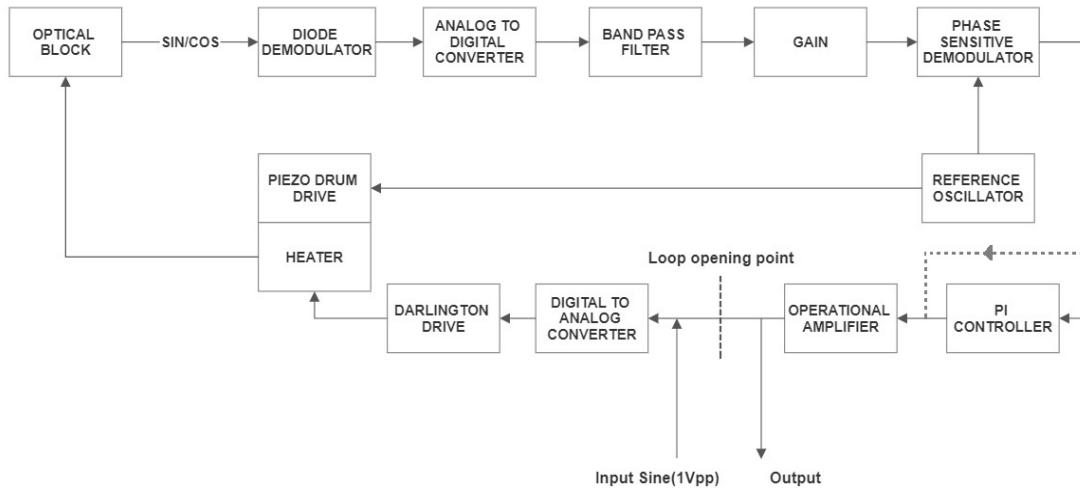


Figure 3.3: Open loop frequency response Block diagram.

Open loop modelling of path length loop for Self-heating

To obtain a system model in open loop mode for the path length control loop, the PI controller is excluded, and a Frequency Response Analyzer (FRA) is employed. The FRA introduces a sine wave input into the gyroscope sensor, and the resulting response is captured and analyzed. The experiment involves incrementally increasing the frequency of the injected sine wave, covering a range of frequencies. This allows for the measurement of the gyroscope's response across different frequency values. The setup is kept stationary for a period of time to allow the gyroscope to self-stabilize and reach a steady state under varying temperatures. The obtained response is referred to as the self-heating response. By analyzing the magnitude and phase data obtained from the FRA, a system model can be developed. Matlab software's system identification toolbox or control system design toolbox can be utilized for this purpose. These tools facilitate the analysis and modelling of the system based on the acquired response data. Using the self-heating response and the system identification tools, researchers can create an accurate model of the path length control loop in the ring laser gyroscope. This model can be further employed for analysis, optimization, and control design, enhancing the understanding and performance of the path length control system.

Closed loop modelling of path length loop for Self-heating

In order to obtain the system model for the path length control loop in closed loop mode, the entire loop is kept closed, including the PI controller. A Frequency Response Analyzer (FRA) is utilized to inject a sine wave into the gyroscope sensor, and the resulting response is cap-

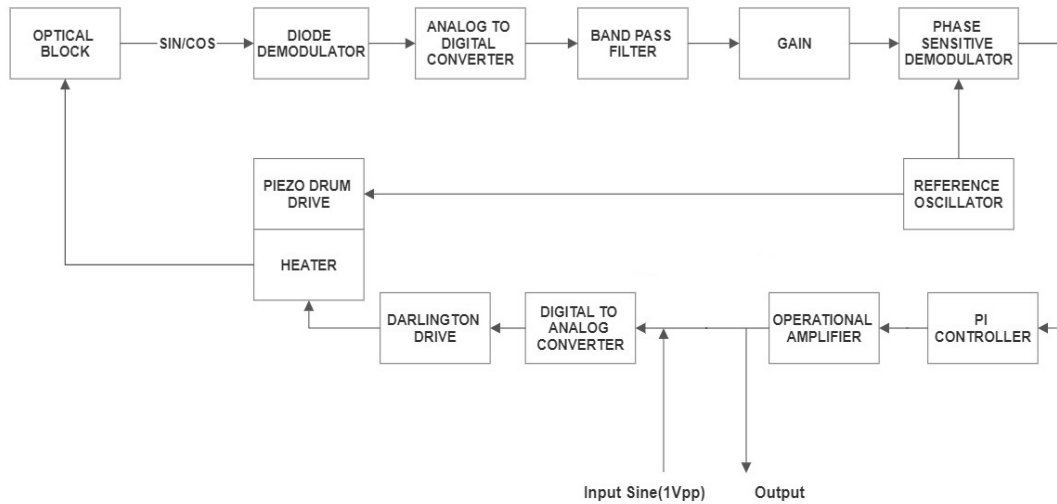


Figure 3.4: Closed loop frequency response Block diagram.

tured and analyzed. To begin the testing, the system is allowed to stabilize by keeping the setup stationary for a certain period of time. Once the system has reached a steady state, a frequency sweep is performed by gradually increasing the frequency of the injected sine wave from a small value to a larger value. This process enables the measurement of the gyroscope's response across a range of frequencies. During the frequency sweep, the response of the system is captured by the FRA. The obtained data, including the magnitude and phase information, is then analyzed using the Matlab toolbox for system identification. Using the Matlab toolbox, the collected response data can be processed and used to generate a mathematical model of the path length control loop. The toolbox offers various techniques, such as frequency domain analysis or system identification algorithms, to derive the model that accurately represents the behaviour of the system. By obtaining and analyzing the system model, we gain a deeper understanding of the path length control loop and make informed decisions regarding its optimization and performance enhancement.

MATLAB toolbox for System identification

The System Identification Toolbox in MATLAB offers a variety of functions, Simulink blocks, and an app that are specifically designed for dynamic system modeling, time-series analysis, and forecasting. This toolbox enables users to estimate the dynamics of nonlinear systems using techniques such as Hammerstein-Wiener and Nonlinear ARX models, as well as machine learning methods like Gaussian Processes and Support Vector Machines. In addition, the toolbox supports the use of deep learning approaches to construct neural ODE models capable of

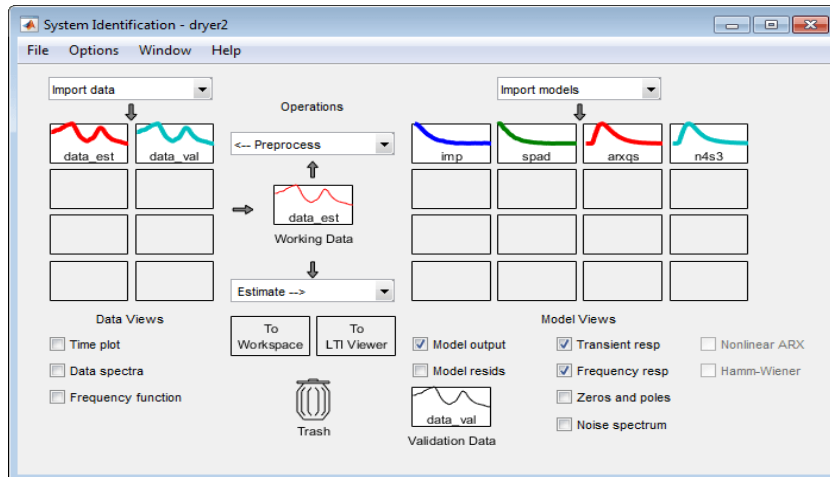


Figure 3.5: System identification toolbox in Matlab.

representing nonlinear system dynamics. It provides flexibility for users to perform grey-box system identification, allowing them to estimate parameters for their own user-defined models. Furthermore, the integration of the identified models into Simulink allows for efficient simulations that can support various applications, including control design, diagnostics, and prognostics. Overall, the System Identification Toolbox provides a comprehensive set of tools that enable users to effectively model and identify system dynamics, facilitating the development of accurate and reliable models for analysis and simulation purposes in Matlab and Simulink environments.[10].

MATLAB toolbox for control system design

Control System Toolbox provides a comprehensive range of tools and techniques for the systematic assessment, design, and optimization of linear control systems. This powerful software package offers various methods for evaluating and fine-tuning control systems. Whether your system is described using a transfer function, state-space, zero-pole-gain, or frequency-response model, Control System Toolbox can effectively handle the specification and analysis of your control system. To evaluate system behavior in both the time and frequency domains, Control System Toolbox provides valuable tools and functions such as the step response plot and Bode plot. These enable us to gain insights into how the system behaves dynamically. For interactive adjustment of compensator settings, two methods offered by Control System Toolbox are Bode loop shaping and the root locus approach. These methods facilitate the fine-tuning of compensators by iteratively modifying their parameters. The toolbox's capabilities extend beyond PID

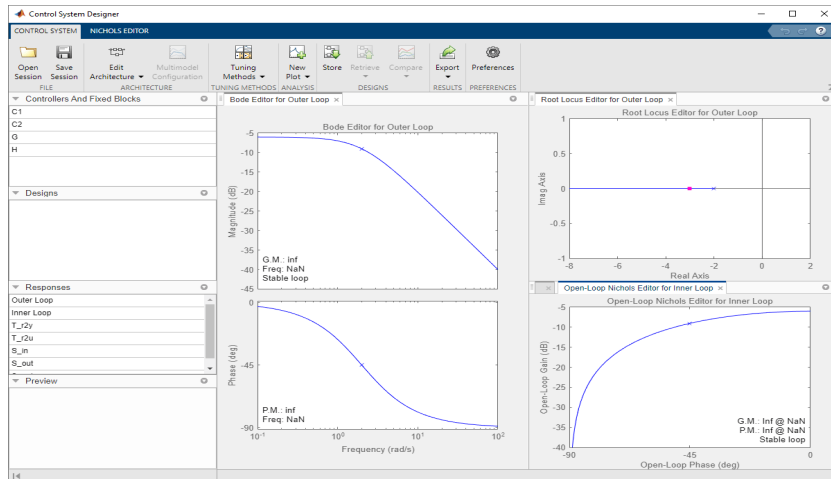


Figure 3.6: Control system design toolbox in Matlab.

controllers and encompass the automatic adjustment of SISO and MIMO compensators. Compensators can comprise multiple adjustable blocks that span various feedback loops, allowing for flexible control system configurations. In addition, the toolbox supports the tuning of gain-scheduled controllers, catering to a diverse range of tuning goals such as reference tracking, disturbance rejection, and stability margins. By verifying parameters such as rising time, overshoot, and settling time, we can effectively validate our control system design and ensure its performance aligns with our objectives.[10].

3.2.3 Thermal sensitivity modelling of path length control loop

In order to investigate the impact of temperature variations on a gyroscope, an experimental setup involving a thermal chamber was utilized. Initially, the system was modelled at room temperature 25°C , and the control loop was designed accordingly. Subsequently, two different temperature scenarios were considered: 60°C and 13°C . These variations were employed to assess the effects of temperature changes on the system's behaviour. When the system was tested in an open-loop configuration, it exhibited characteristics that could be accurately represented by a second-order system model. However, when tested in a closed-loop configuration, the system displayed behaviour that could be more adequately captured by a third-order system model. Notably, the coefficients of the transfer functions differed from those observed under normal room temperature conditions. This observation indicates that temperature fluctuations exert a significant influence on the performance of the path length control system, leading to notable changes in its underlying model.



Figure 3.7: Thermal chamber for various temperature tests.

3.3 CONTROL SYSTEM DESIGN

3.3.1 Model Reference Adaptive PID Control

Adaptive control is a branch of control systems engineering that deals with the design and implementation of control algorithms capable of adjusting their parameters in real-time to adapt to changes in the system or its environment. The objective of adaptive control is to enhance the performance and robustness of control systems by continuously updating the controller parameters based on online measurements and system dynamics. In adaptive control, there are typically two main components: the controller and the adaptation mechanism.

- **Controller:** The controller is responsible for generating control signals to drive the system towards a desired behavior or setpoint. It can be a classical controller like a PID controller or a more sophisticated model-based controller. The controller's parameters, such as gains or coefficients, may initially be set based on system knowledge or design criteria.
- **Adaptation Mechanism:** The adaptation mechanism continuously monitors the system's behavior and adjusts the controller parameters to improve control performance. This mechanism relies on real-time measurements and estimation techniques to identify the system's dynamics and update the controller parameters accordingly. The adaptation process can be based on various approaches, such as model reference adaptive control, gain scheduling, or reinforcement learning.

The key idea behind adaptive control is to enable the control system to handle uncertainties, variations, and disturbances that are inherent in many real-world systems. By adapting the controller parameters based on online information, adaptive control allows for improved tracking of setpoints, rejection of disturbances, and robustness against system changes. The adaptive control system is specifically intended to work in an environment that fluctuates. As a result, it may assess the process's performance and make changes to get the desired outcome. An adaptive control block diagram is given as,

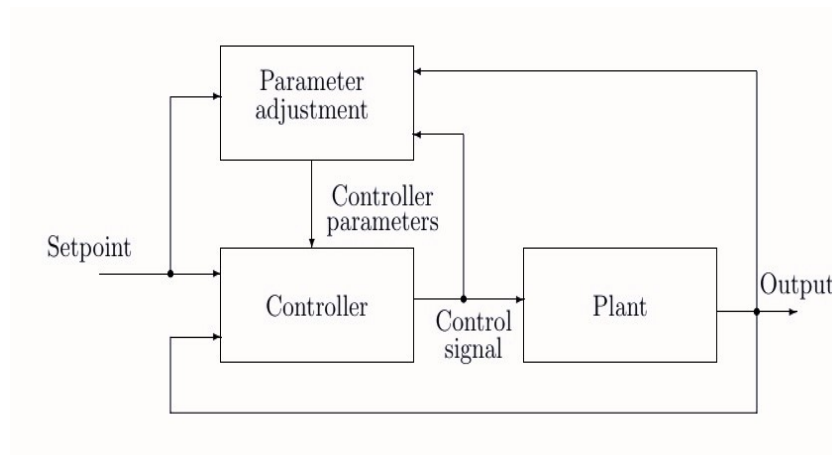


Figure 3.8: Adaptive control Block diagram.

In the context of the system being discussed, the utilization of adaptive control becomes essential due to the possibility of varying working conditions, including temperature changes. It is crucial to ensure the system's stability under different temperatures, even those deviating from the normal room temperature. The system needs to be capable of adapting to these changing environments while maintaining stable operation. This project employs the approach of adaptive control, which involves incorporating a reference model. Utilizing this reference model allows the system to adapt to unfavourable conditions and maintain its performance accordingly. The model reference adaptive control(MRAC) is depicted as follows,

Model Reference Adaptive Control (MRAC) is a control technique that aims to achieve a desired system behavior by comparing it to a reference model. It is particularly useful in scenarios where the system dynamics may vary or be uncertain. In MRAC, a reference model is established to represent the desired response of the system. The controller continually adjusts its parameters in order to minimize the disparity between the actual system output and the output of the reference model. This adaptive adjustment allows the controller to compensate for uncertainties or changes in the system dynamics. The adaptation mechanism in MRAC typically

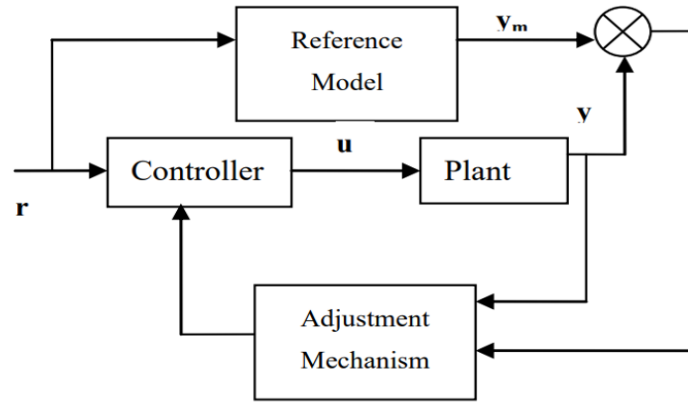


Figure 3.9: Model Reference Adaptive control Block diagram.

involves online estimation or identification of the system parameters using appropriate algorithms. These algorithms utilize the input-output data of the system to update the controller parameters and align the system's behavior with the reference model. The key advantage of MRAC lies in its capability to handle systems with time-varying or uncertain dynamics. By continuously updating the control parameters based on real-time information, MRAC can adapt to changes in the system and provide improved performance and stability, even in the presence of disturbances or variations in operating conditions. It offers a robust and versatile control approach that ensures the controlled system closely tracks the desired reference model, regardless of variations or uncertainties in the system dynamics.

The reference model considered in this control design is the path length control closed loop system working under the normal temperature of 25°C, ie.

$$\frac{0.02S + 3.4}{S^3 + 4.8S^2 + 5.9S + 3.4} \quad (3.1)$$

The plant model considered for control is the same closed path length control loop at a higher temperature of 60°C, ie.

$$\frac{13.66S + 2.771}{S^3 + 7.414S^2 + 12.52S + 2.771} \quad (3.2)$$

Design of Adaptive control parameters

The design of adaptation parameters for adaptive control depends on the specific adaptive control algorithm being used. Here are some general considerations and approaches for adaptation parameter design:

1. Lyapunov-Based Design:

- If employing a Lyapunov-based approach, the adaptation parameters can be designed based on the Lyapunov stability analysis.
- The adaptation law should ensure that the Lyapunov function or its derivative decreases over time, guaranteeing stability and convergence.
- The specific form of the adaptation law will depend on the Lyapunov function and the system dynamics.

2. Gradient-Based Design:

- Gradient-based adaptation methods often involve estimating the gradient of a performance cost function with respect to the adaptation parameters.
- The adaptation parameters are updated based on the gradient estimation and a step size (learning rate).
- The choice of the performance cost function and gradient estimation method depends on the specific control problem and available information about the system.

3. Recursive Least Squares (RLS):

- In the case of adaptive control algorithms utilizing RLS, the adaptation parameters are updated recursively using a weighted least squares estimation.
- The weighting factors determine the trade-off between tracking performance and parameter estimation accuracy.
- The design of the weighting factors can be based on the desired control performance and the noise characteristics of the system.

4. Model-Based Design:

- If the adaptive control algorithm is based on a model of the system, the adaptation parameters can be designed by considering the model's characteristics.
- The parameters may be chosen to reflect the desired convergence rate, stability margins, or robustness properties.
- Model-based design often involves analyzing the closed-loop system stability and performance using control theory techniques.

5. Trial-and-Error and Tuning:

- In practice, adaptation parameters are often fine-tuned through experimental or simulation-based trials.
- Start with initial parameter values and observe the system's behavior.
- Adjust the adaptation parameters based on the observed performance until satisfactory tracking, stability, and robustness are achieved.

Lyapunov stability based Adaptive control design

The system considered as model and reference in this project is of third order system. To analyze the stability of a third-order system using Lyapunov stability, we need to define a Lyapunov function and examine its derivative along the system trajectories. Consider a third-order nonlinear system described by the differential equation:

$$\dot{x} = f(x) \quad (3.3)$$

where x is the state vector of the system, and $f(x)$ represents the dynamics of the system.

To apply Lyapunov stability analysis, we choose a Lyapunov function $V(x)$ that satisfies the following properties:

- $V(x) > 0$ for all x except at origin.
- $V(0) = 0$ at the origin.
- $\dot{V}(x) = \frac{dV(x)}{dt}$ is negative definite or negative semidefinite, meaning that $\dot{V}(x) \leq 0$ for all x except at origin.

The negative definiteness or negative semidefiniteness of $\dot{V}(x)$ guarantees that the Lyapunov function is decreasing or non-increasing along the system trajectories, except at the origin. This implies stability properties for the system.

To determine the stability of the third-order system, we need to compute the time derivative of the Lyapunov function,

$$\dot{V}(x) = \frac{dV(x)}{dt} \quad (3.4)$$

Substituting the system dynamics, $\dot{x} = f(x)$, we have:

$$\dot{V}(x) = \frac{dV(x)}{dt} f(x) \quad (3.5)$$

If we can find a Lyapunov function such that $\dot{V}(x) < 0$ for all x except at the origin, then the system is globally asymptotically stable. If $\dot{V}(x) \leq 0$ for all x except at the origin, then the system is stable but not necessarily asymptotically stable. It is important to note that finding a suitable Lyapunov function can be a challenging task, especially for higher-order systems. The choice of Lyapunov function often involves trial and error or depends on the specific system's dynamics. Different Lyapunov functions may lead to different stability conclusions. Additionally, Lyapunov stability analysis for higher-order systems can become more complex due to the increased dimensionality and potential presence of multiple equilibrium points. Advanced techniques, such as LaSalle's invariance principle or input-to-state stability, may be needed to analyze stability in these cases.

To analyze the stability of a third-order system using Lyapunov stability, we need to define a Lyapunov function and examine its derivative along the system trajectories. The negative definiteness or negative semidefiniteness of the derivative implies stability properties for the system. However, finding an appropriate Lyapunov function can be challenging, and higher-order systems may require more advanced analysis techniques.

Considering the first order system given in fig (3.10),

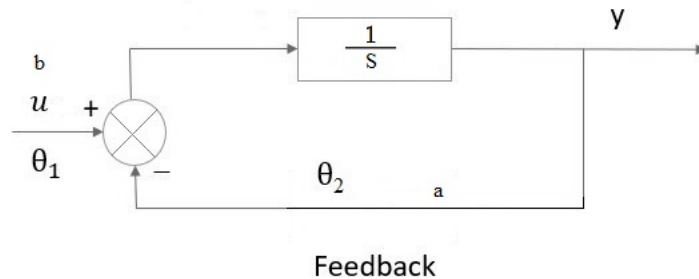


Figure 3.10: Feedback Control system.

The reference model is represented as,

$$\frac{dy_m}{dt} = -a_m y_m + b_m u_c \quad (3.6)$$

The plant model is represented as,

$$\frac{dy}{dt} = -ay + bu \quad (3.7)$$

where a and b are unknown and $b > 0$.

The control law can be,

$$u = \theta_1 u_c - \theta_2 y \quad (3.8)$$

Equation (3.3) in (3.2)

$$\dot{y} = -ay + b(\theta_1 u_c - \theta_2 y) \quad (3.9)$$

$$(-a - b\theta_2)y + b\theta_1 u_c \quad (3.10)$$

The error,

$$e = y - y_m \quad (3.11)$$

$$\dot{e} = \dot{y} - \dot{y}_m \quad (3.12)$$

$$\dot{e} = (-a - b\theta_2)y + b\theta_1 u_c + a_m y_m - b_m u_c \quad (3.13)$$

$$\dot{e} = -a_m(y - y_m) + (a_m - a - b\theta_2)y + (b\theta_1 - b_m)u_c \quad (3.14)$$

$$\dot{e} = -a_m e + (a_m - a - b\theta_2)y + (b\theta_1 - b_m)u_c \quad (3.15)$$

Considering candidate Lyapunov's function,

$$V = \frac{1}{2}e^2 + \frac{1}{2\gamma b}(a_m - a - b\theta_2)^2 + \frac{1}{2\gamma b}(b\theta_1 - b_m)^2 \quad (3.16)$$

The derivative of the candidate Lyapunov's function,

$$\dot{V} = e\dot{e} = -\frac{1}{\gamma b}(a_m - a - b\theta_2)b\dot{\theta}_2 + \frac{1}{\gamma b}(b\theta_1 - b_m)b \quad (3.17)$$

Considering equation (3.10) in (3.12),

$$\dot{V} = e(-a_m e + (a_m - a - b\theta_2)y + (b\theta_1 - b_m)u_c) - \frac{1}{\gamma}(a_m - a - b\theta_2)\dot{\theta}_2 + \frac{1}{\gamma}(b\theta_1 - b_m)\dot{\theta}_1 \quad (3.18)$$

For \dot{V} to be negative semi-definite, $\dot{\theta}_2$ and $\dot{\theta}_1$ should be as follows,

$$\dot{\theta}_2 = \gamma e y \quad (3.19)$$

$$\dot{\theta}_1 = -\gamma e u_c \quad (3.20)$$

where γ is the adaptation parameter and θ is the control input parameter[11].

MIT rule-based Adaptive control design

This method is developed by the Massachusetts Institute of Technology, named as MIT rule which proposes a cost function of error and the development of an algorithm for the reduction of it[12].

We can consider the same system as described above, ie.

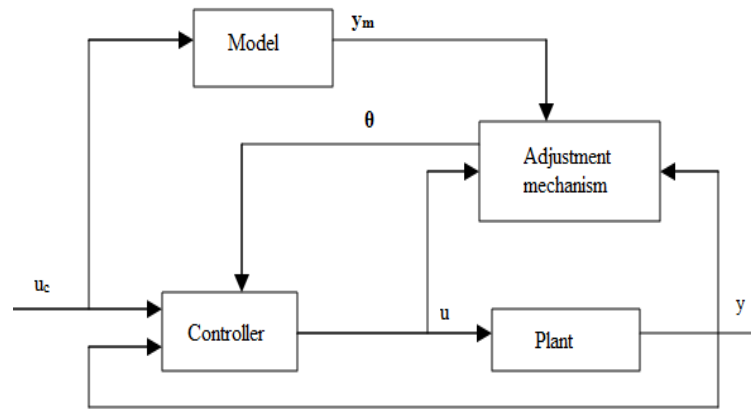


Figure 3.11: Model Reference Adaptive Control method.

$$\frac{dy}{dt} = -ay + bu \quad (3.21)$$

where a and b are unknown and $b > 0$.

a and b are the parameters which specify the dynamics of the system. As usual, the reference model is to be defined.

$$\frac{dy_m}{dt} = -a_m y_m + b_m u_c \quad (3.22)$$

In the reference model, the parameters a_m and b_m are the dynamics of the reference model which is known. u_c is the input to the reference model.

The control input $u(t)$ has to be established.

$$u(t) = \theta_1(t)u_c(t) - \theta_2(t)y(t) \quad (3.23)$$

The parameter θ is an adaptive control parameter determined by an adaptive control algorithm. The objective is to make output of system as close as the output of the model by means of adjusting θ .

By substituting control law in the system equation, we get closed-loop system as

$$\frac{dy}{dt} = -(a + b\theta_2)y + b\theta_1 u_c \quad (3.24)$$

By comparing this equation with reference model, the parameters θ_1 should be $\frac{b_m}{b}$ and θ_2 should be $\frac{a_m - a}{b}$ respectively for getting system similar to reference model. The hindrance of getting value of θ is the unknown a and b . For getting an optimised value of θ , consider the following cost function.

$$J = \frac{1}{2}e^2 \quad (3.25)$$

The e mentioned in the cost function is error term which can be represented as,

$$e(t) = y(t) - y_m(t) \quad (3.26)$$

The way to decrease the error is to minimise θ in the direction of negative gradient of J .

$$\frac{d\theta_1}{dt} = -\alpha \frac{\partial J}{\partial \theta_1} = -\alpha e \frac{\partial e}{\partial \theta_1} \quad (3.27)$$

$$\frac{d\theta_2}{dt} = -\alpha \frac{\partial J}{\partial \theta_2} = -\alpha e \frac{\partial e}{\partial \theta_2} \quad (3.28)$$

For finding partial fractions of $\frac{\partial e}{\partial \theta_1}$ and $\frac{\partial e}{\partial \theta_2}$, a new operator g is introduced.

$$gf(t) \equiv \frac{df(t)}{dt} \quad (3.29)$$

From equation(3.24), we get,

$$gy = -(a + b\theta_2)y + b\theta_1 u_c \quad (3.30)$$

$$(g + a + b\theta_2)y = b\theta_1 u_c \quad (3.31)$$

$$y = \frac{b\theta_1 u_c}{g + a + b\theta_2} \quad (3.32)$$

The error term e can be written in terms of y as,

$$e = \frac{b\theta_1 u_c}{g + a + b\theta_2} - y_m \quad (3.33)$$

Taking partial derivatives with respect to θ_1 and θ_2 ,

$$\frac{\partial e}{\partial \theta_1} = \frac{b u_c}{g + a + b\theta_2} \quad (3.34)$$

$$\frac{\partial e}{\partial \theta_2} = \frac{-by}{g + a + b\theta_2} \quad (3.35)$$

Thus partial derivatives were found. Since it depends on a and b , again we have to consider an ideal case where $a_m \approx a + b\theta_2$ thereby $g + a + b\theta_2 \approx p + a_m$

Substituting equations (3.34) and (3.35) in equations (3.27) and (3.28) respectively and the expression for parameter change is given as,

$$\frac{d\theta_1}{dt} = -\frac{b}{a_m} \cdot \frac{a_m u_c}{p + a_m} e = -\gamma \frac{a_m u_c}{p + a_m} e \quad (3.36)$$

$$\frac{d\theta_2}{dt} = \alpha \frac{b}{a_m} \cdot \frac{a_m y}{p + a_m} e = \gamma \frac{a_m y}{p + a_m} e \quad (3.37)$$

The coefficient $\frac{\alpha b}{a_m}$ is the parameter gain[13]. Here, a PID controller tuned with Matlab PID tuner toolbox is used as a compensator to which the adaptive parameters are added for tracking the reference[14].

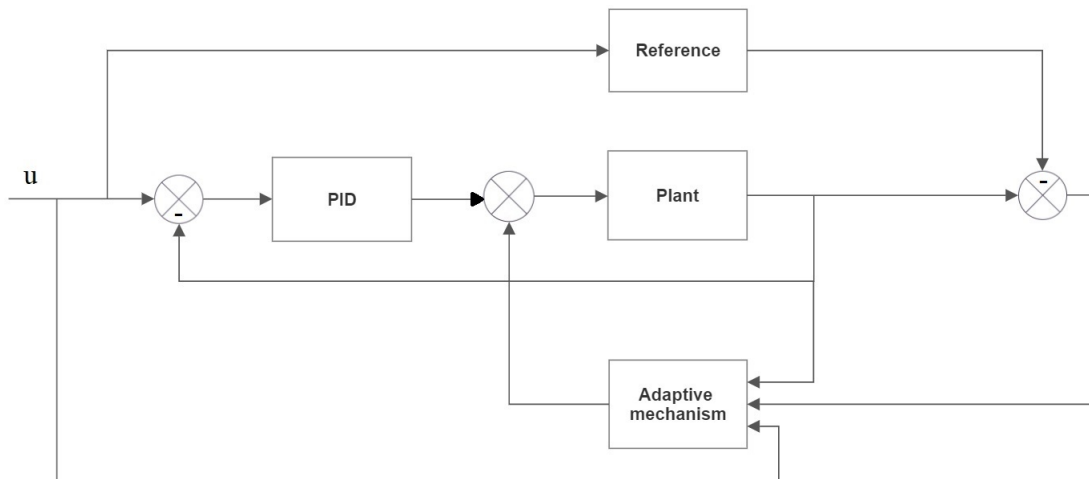


Figure 3.12: Simulation block diagram of proposed model reference adaptive control.

3.4 SUMMARY

This chapter explained the method for constructing a self-heating model to determine the path length in a ring laser gyroscope. The model was established by operating the gyroscope under normal temperature conditions and studying the path length control loop. Subsequently, the gyroscope was subjected to tests at both higher and lower temperatures, resulting in the development of temperature-dependent models. These models were utilized to evaluate the effects of temperature variations on the system and to devise suitable control corrections. The findings demonstrated that temperature fluctuations have a substantial impact on the gyroscope's performance. To address this issue, adaptive control techniques using model referencing were simulated for implementing corrective measures.

Chapter 4

RESULTS

4.1 OVERVIEW

The path length control loop of the ring laser gyroscope plays a crucial role in ensuring accurate angular rate measurement by operating the laser at its optimal gain peak. However, changes in temperature can significantly impact the laser's performance at this operating point. To maintain stability in the path length control loop regardless of temperature fluctuations, it is essential to incorporate corrective measures. An adaptive approach is employed, where a model is utilized as a reference in the outer loop of the path length control system. This adaptive method aids in implementing the aforementioned corrections. The frequency response of the path length control loop is utilized for mathematical modelling purposes. The results of the mathematical modelling, including closed loop and open loop responses under different band pass filter gains are included in this section. To address the correction requirements of the path length control loop, a model reference adaptive control strategy is employed. The simulation results, showcasing the effectiveness of the control strategy, are also depicted.

4.2 RESULTS

4.2.1 Frequency responses of path length control loop in open and closed loop conditions for various band pass filter gains

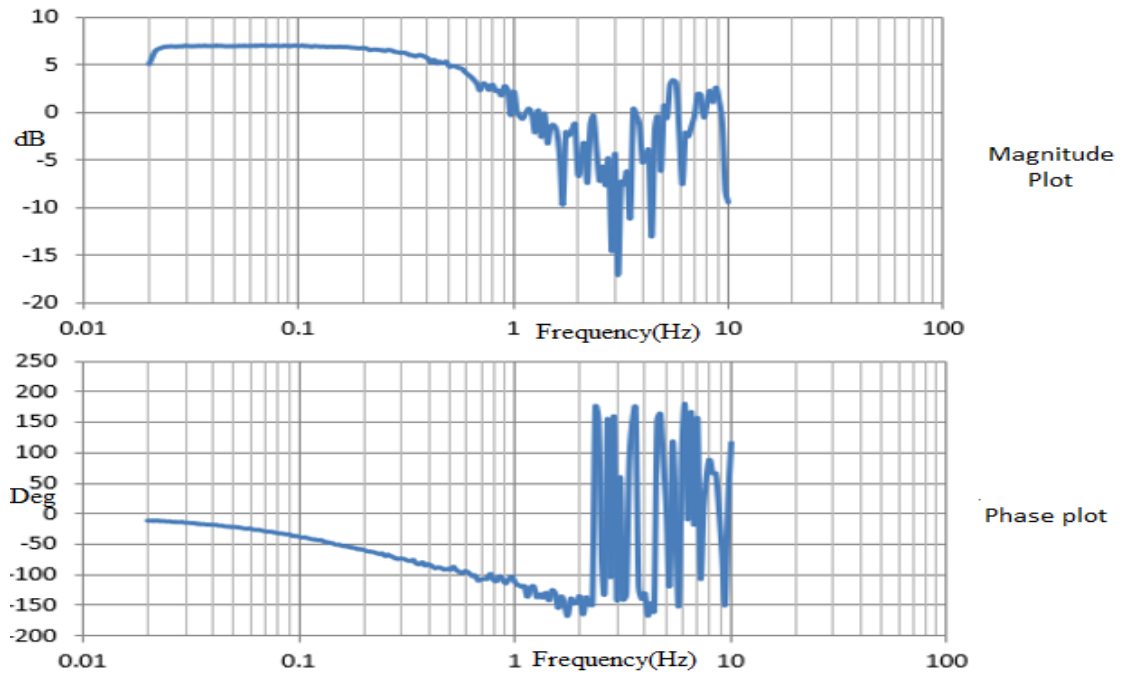


Figure 4.1: Experimental frequency response plot of open loop system for bandpass filter gain 5.

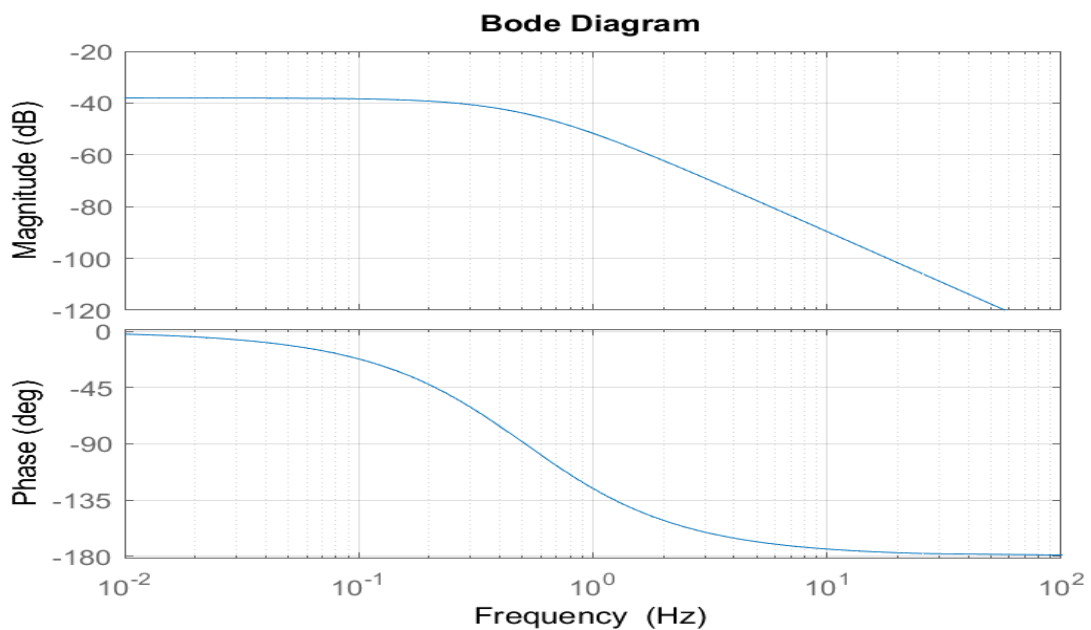


Figure 4.2: Frequency response plot of open loop system for bandpass filter gain 5 generated with Matlab.

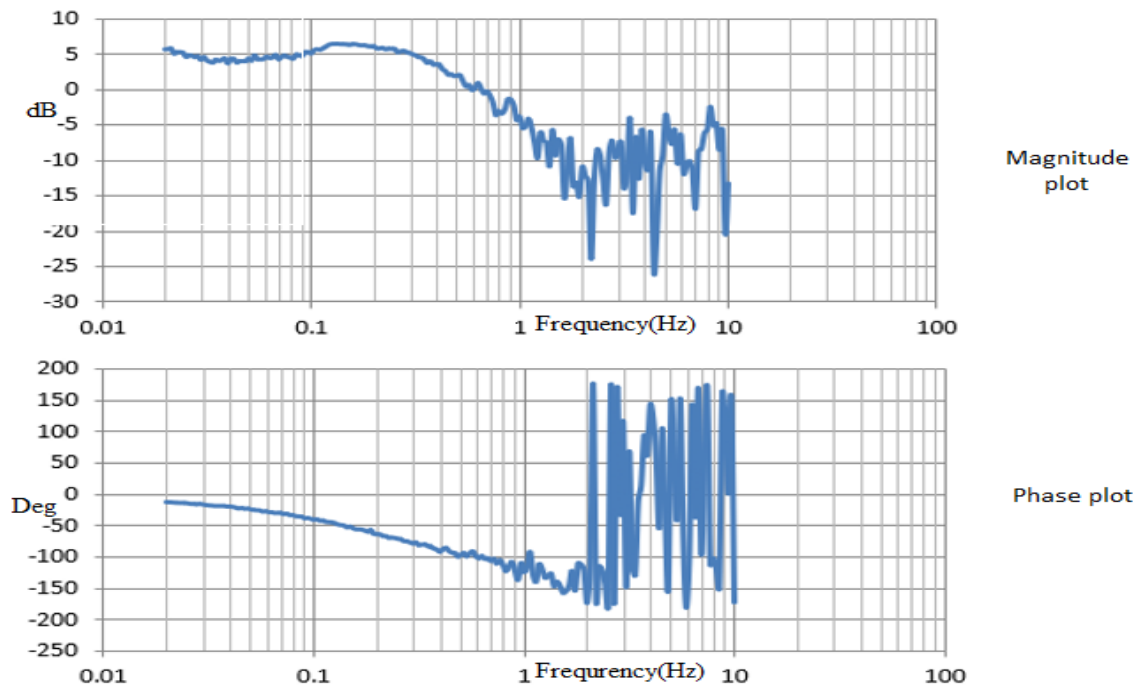


Figure 4.3: Experimental frequency response plot of open loop system for bandpass filter gain 10.

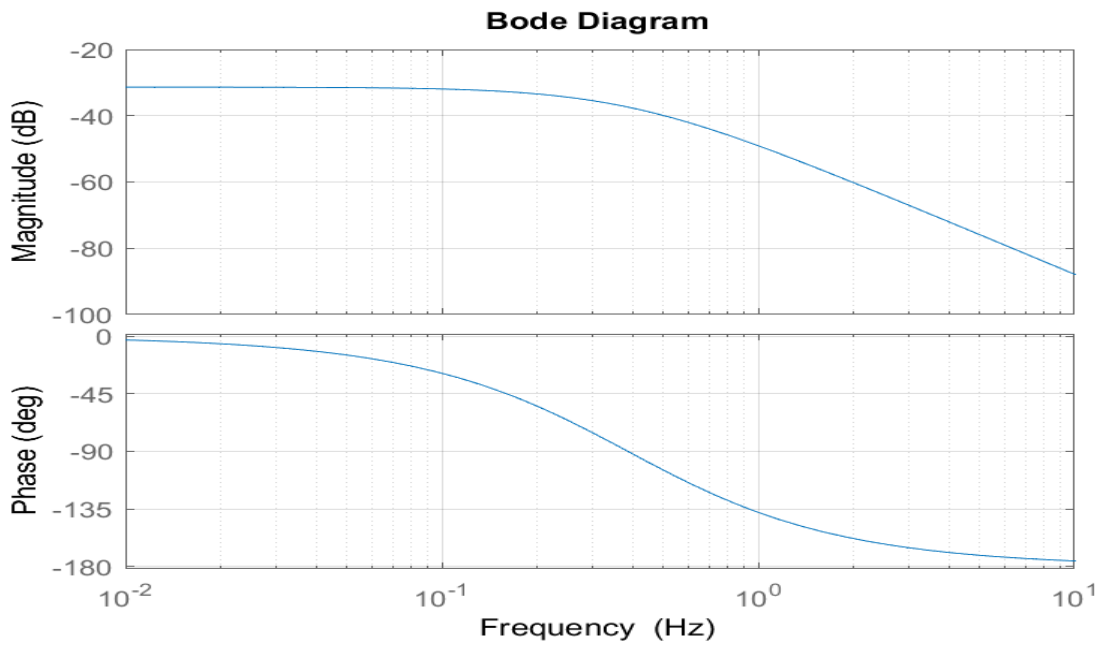


Figure 4.4: Frequency response plot of open loop system for bandpass filter gain 10 generated with Matlab.

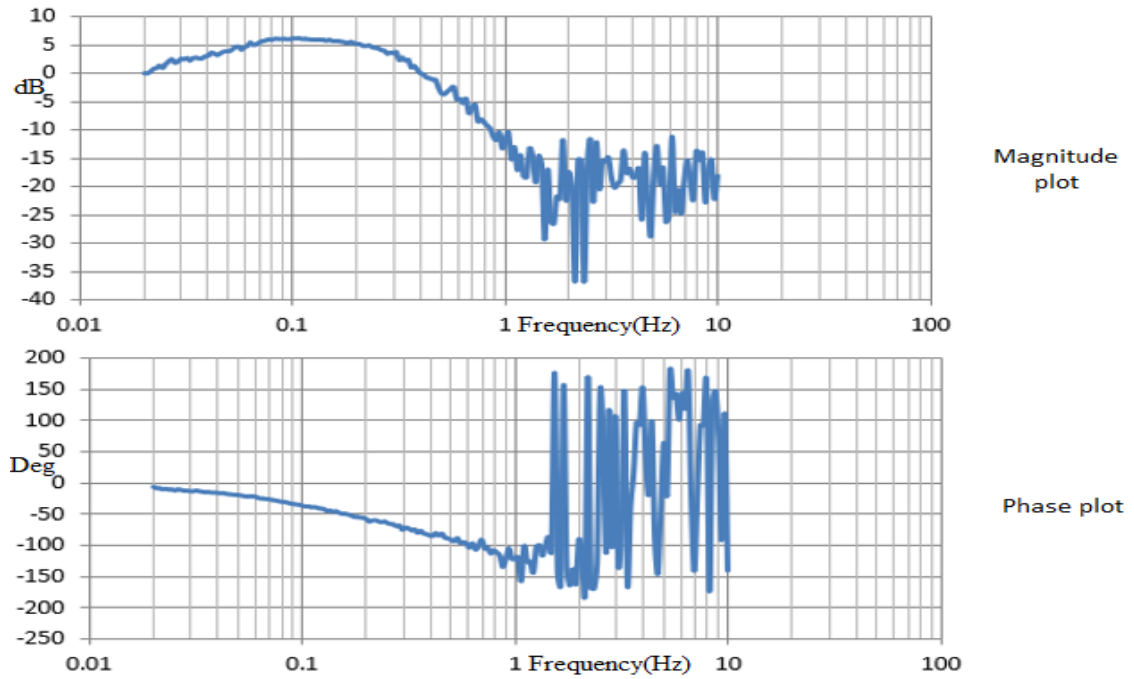


Figure 4.5: Experimental frequency response plot of open loop system for bandpass filter gain 15.

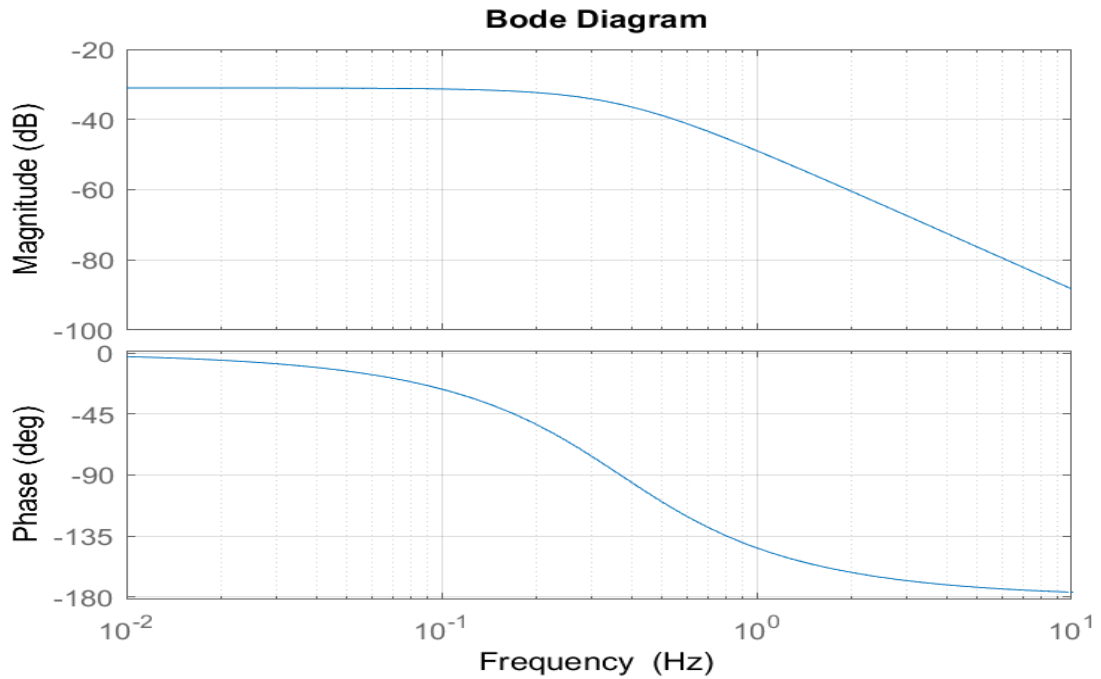


Figure 4.6: Frequency response plot of open loop system for bandpass filter gain 15 generated with Matlab.

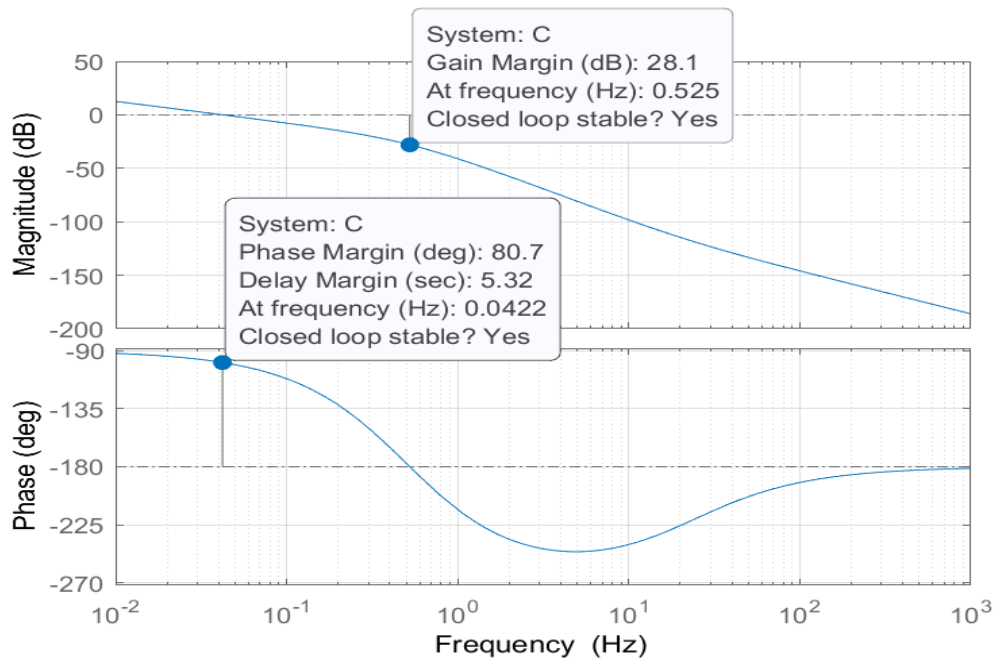


Figure 4.7: Frequency response plot of open loop system with PI controller in series, for bandpass filter gain 5.

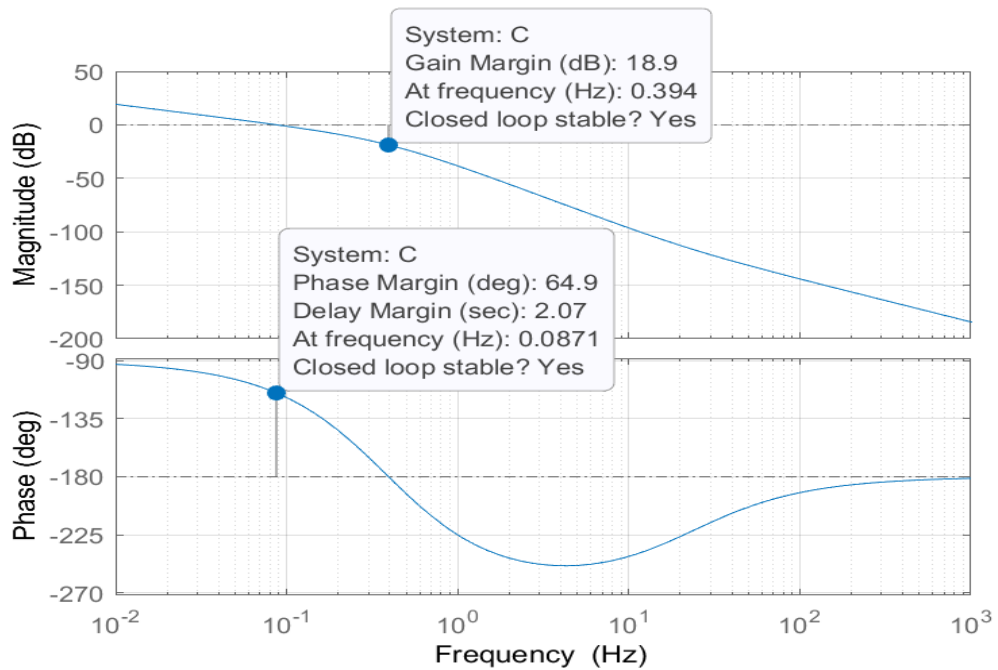


Figure 4.8: Frequency response plot of open loop system with PI controller in series, for bandpass filter gain 10.

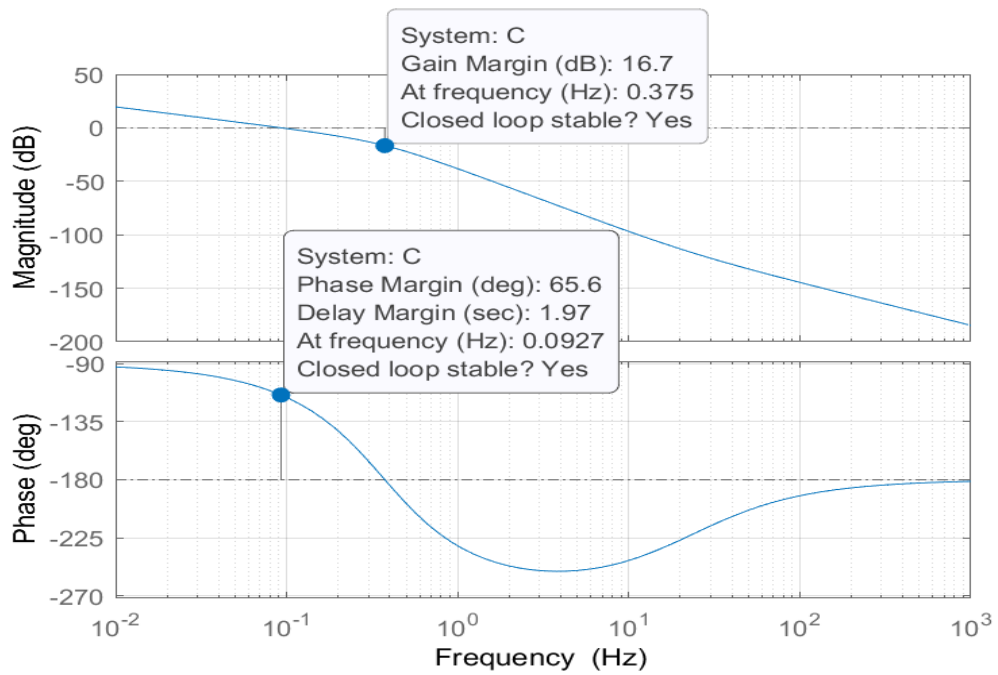


Figure 4.9: Frequency response plot of open loop system with PI controller in series, for bandpass filter gain 15.

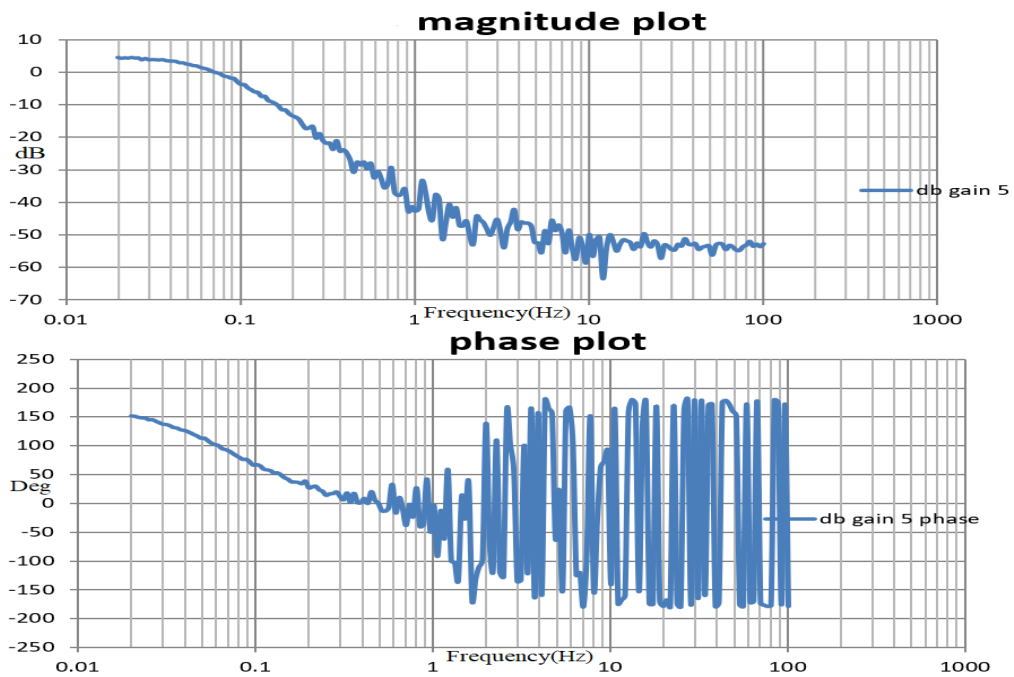


Figure 4.10: Experimental frequency response plot of closed loop system for bandpass filter gain 5.

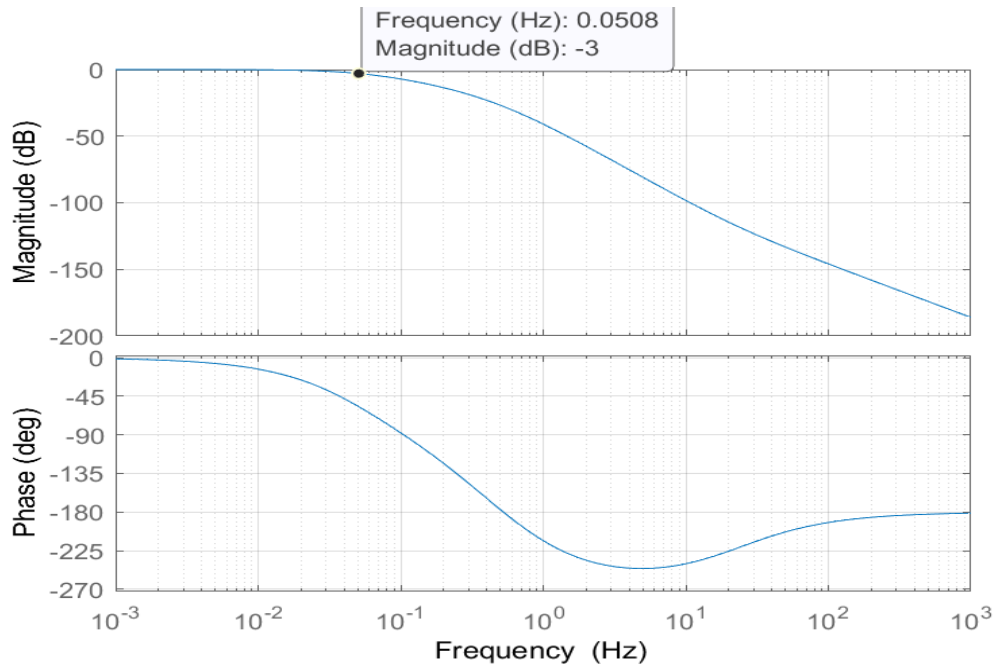


Figure 4.11: Frequency response plot of closed loop system for bandpass filter gain 5 generated with Matlab.

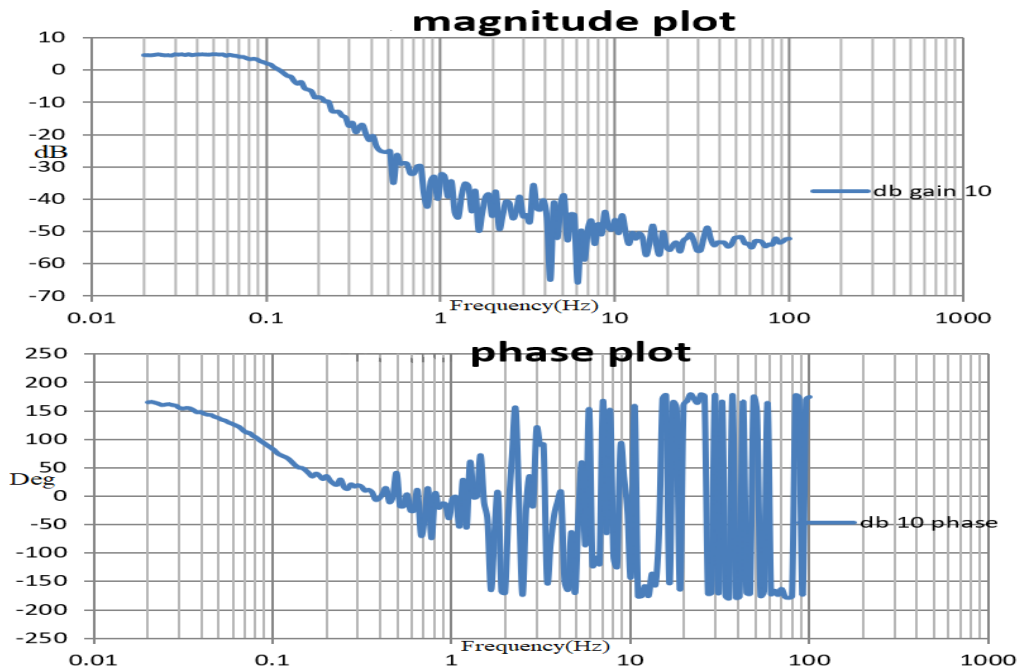


Figure 4.12: Experimental frequency response plot of closed loop system for bandpass filter gain 10.

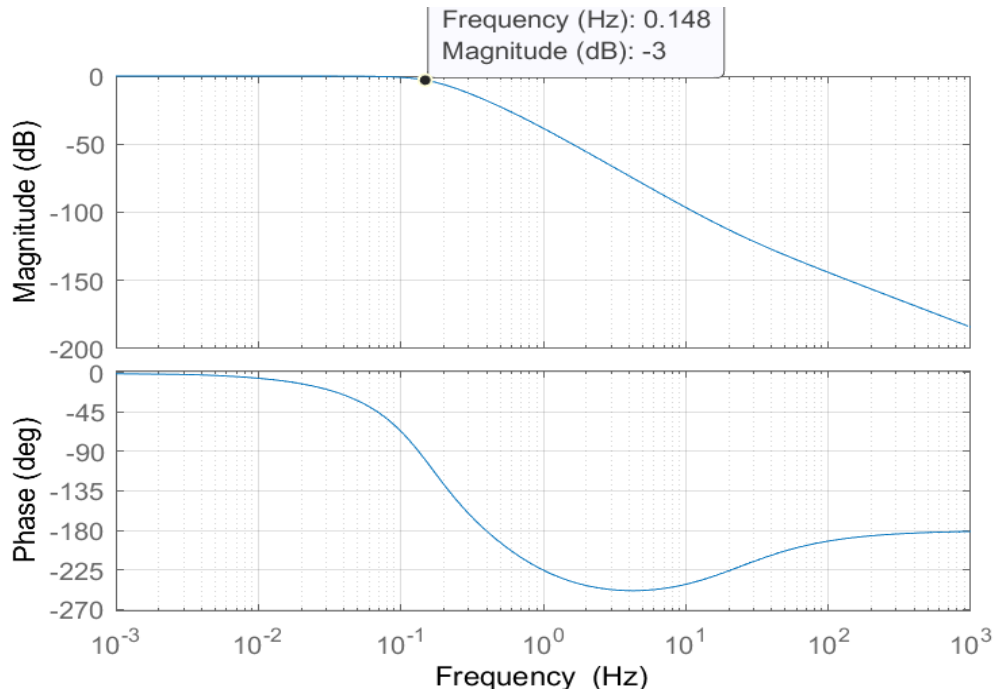


Figure 4.13: Frequency response plot of closed loop system for bandpass filter gain 10 generated with Matlab.

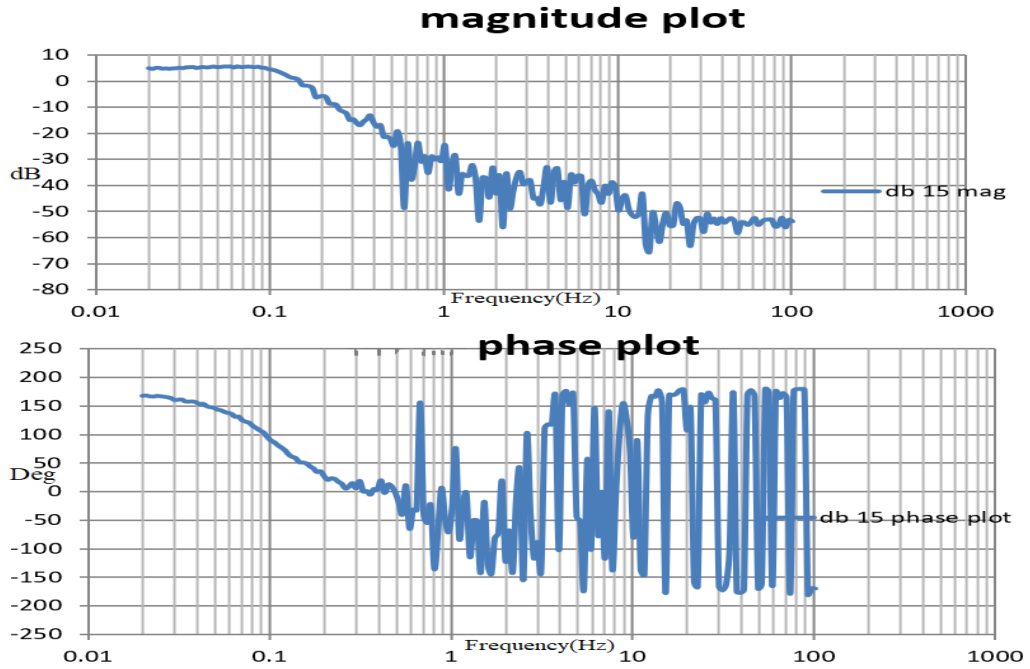


Figure 4.14: Experimental frequency response plot of closed loop system for bandpass filter gain 15.

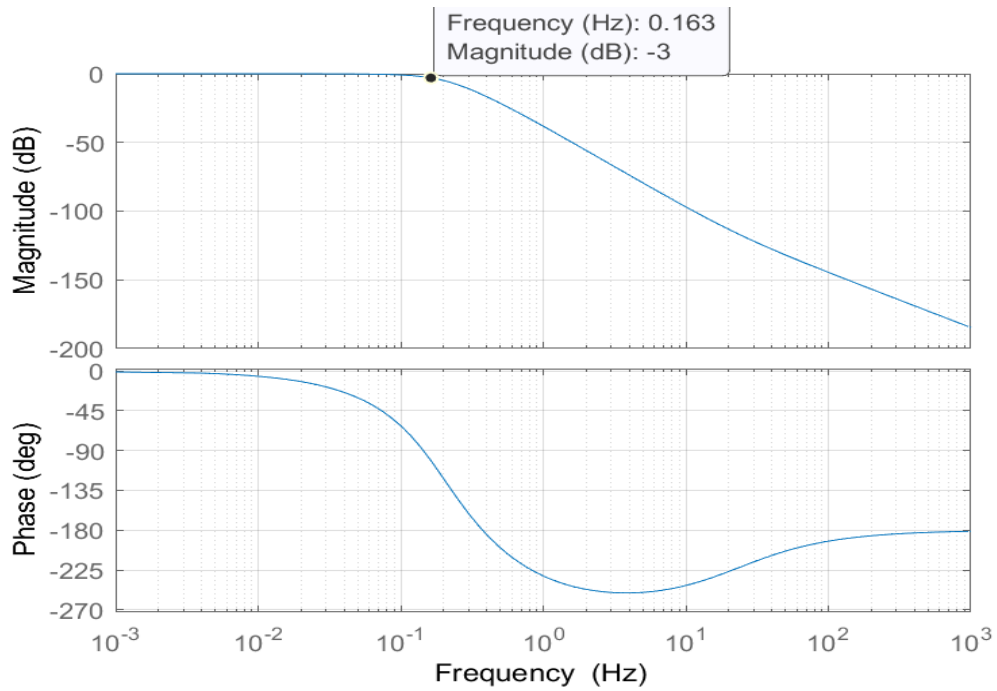


Figure 4.15: Frequency response plot of closed loop system for bandpass filter gain 15 generated with Matlab.

Sensor type	Bpf gain	Gain margin(dB)	Phase margin($^{\circ}$)	Closed loop band width(Hz)
R55	5	28.1	80.7	0.0509
	10	18.9	64.9	0.149
	15	16.7	65.6	0.163
R65	5	27.1	75.2	0.0805
	10	26.4	77.2	0.0697
	15	17.3	70	0.122

Table 4.1: Stability margins from bode plots.

The bandwidth of the system increased when the bandpass filter gain is increased. Two heater load resistances were tested.

4.2.2 Mathematical models derived from frequency responses

Type	OL/ CL	Bpf gain 5	Bpf gain 10	Bpf gain 15
R55	OL	$\frac{0.13}{S^2+6.44S+10.37}$	$\frac{0.16}{S^2+4.867S+5.923}$	$\frac{0.152}{S^2+3.976S+5.39}$
	CL	$\frac{0.02S+2.8}{S^3+6.4S^2+10.3S+2.8}$	$\frac{0.02S+3.4}{S^3+4.8S^2+5.9S+3.4}$	$\frac{0.02S+3.3}{S^3+3.9S^2+5.4S+3.3}$
R65	OL	$\frac{0.20}{S^2+8.07S+11.27}$	$\frac{0.16}{S^2+6.76S+10.02}$	$\frac{0.102}{S^2+3.38S+4.55}$
	CL	$\frac{0.03S+4.4}{S^3+8S^2+11.3S+4.36}$	$\frac{0.02S+3.4}{S^3+6.7S^2+10S+3.48}$	$\frac{0.01S+2.2}{S^3+3.38S^2+4.6S+2.2}$

Table 4.2: Mathematical models derived using control system toolbox.

Mathematical models were estimated for two different heater load resistances of 55 and 66 ohms. For each condition, tests were conducted for getting frequency response.

4.2.3 Validation of mathematical model using Step response

The mathematical model's validation can be ensured by taking a step response. By comparing experimental and theoretical step responses, the similarity between both shows the correctness of the mathematical model. A step signal that has a magnitude of 1V for the +/- 15 voltage range is used to test the model.

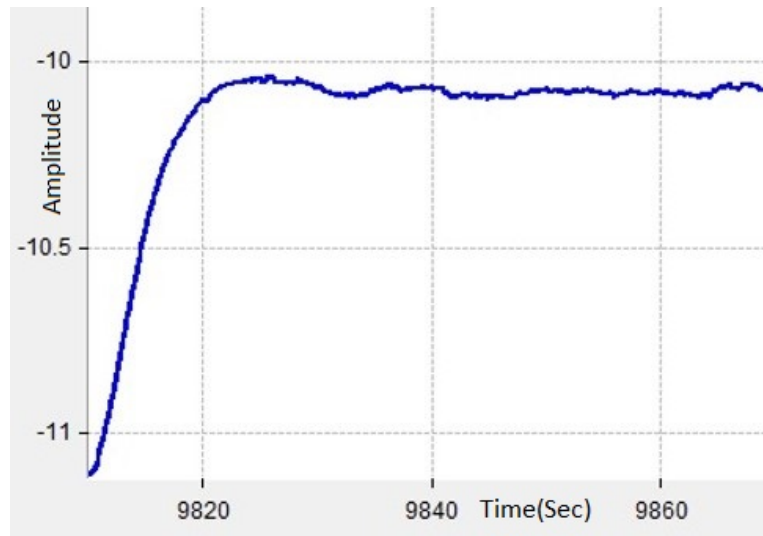


Figure 4.16: Experimental step response.

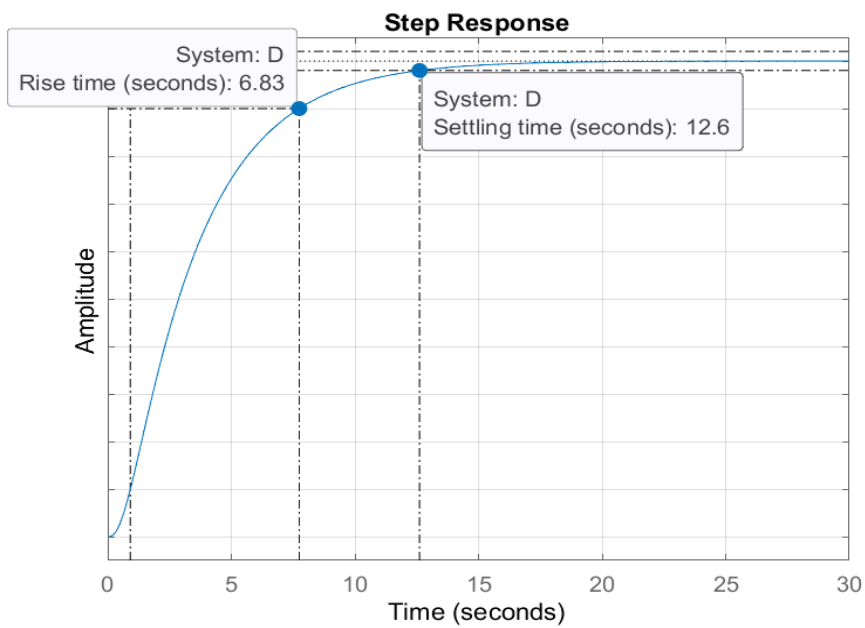


Figure 4.17: Step response generated from Matlab using theoretical model for bandpass filter gain 5

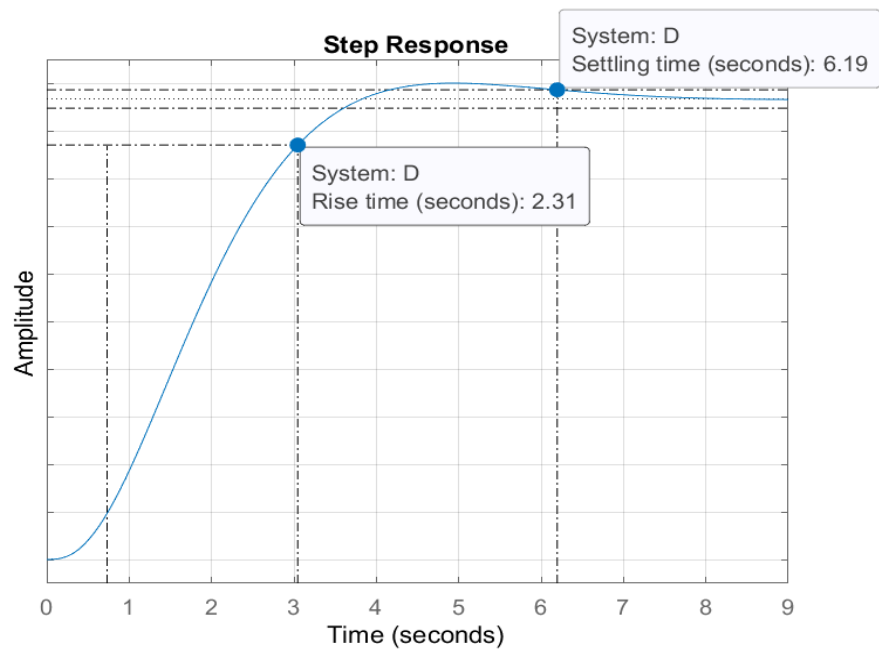


Figure 4.18: Step response generated from Matlab using theoretical model for bandpass filter gain 10

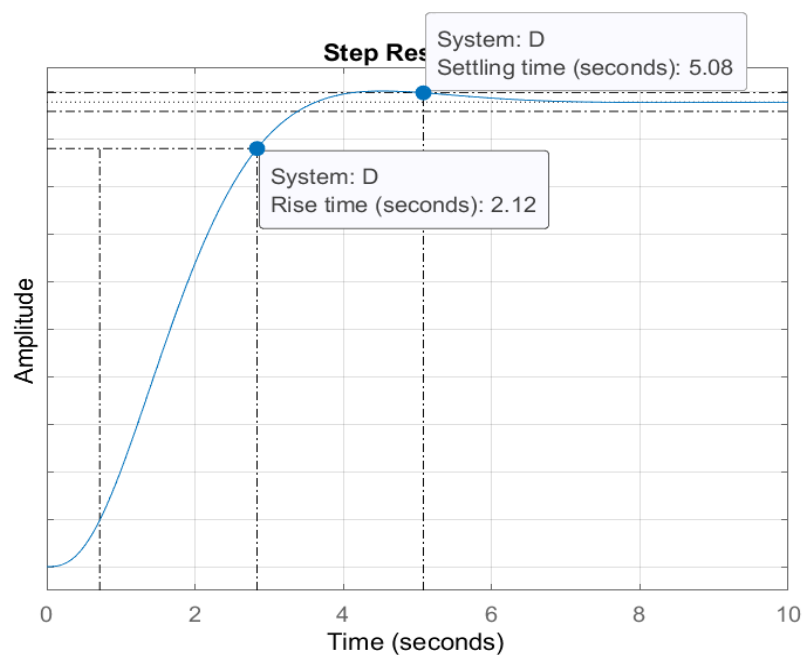


Figure 4.19: Step response generated from matlab using theoretical model for bandpass filter gain 15

Theoretical step responses might be different from actual step responses but there occur similarities if both are of the same mathematical model. A comparison of theoretical and actual step responses is found.

Type	Bpf gain	Settling time(S)	Rise time(S)
R55	5	12.3	6.63
	10	6.19	2.25
	15	5.19	2.06
R65	5	7.29	4.12
	10	8.78	4.79
	15	4.73	2.7

Table 4.3: Theoretical step response parameters.

Type	Bpf gain	Settling time(S)	Rise time(S)
R55	5	12.99	7.2
	10	8.7	3.83
	15	8.55	3
R65	5	11.18	5.82
	10	10.21	4.79
	15	6.67	2.7

Table 4.4: Actual step response parameters.

Type	Bpf gain	Settling time(S)	Rise time(S)
R55	5	10.88	6.86
	10	8.34	3.8
	15	9.3	3.1
R65	5	13	8
	10	10.98	4.82
	15	7.5	3.52

Table 4.5: Phase offset actual step response parameters.

The theoretical step response is found by simulating theoretical mathematical models, and the actual step response is found by experiments. Phase offset response is found by giving an offset to the existing control voltage signal. By the similarities in theoretical and actual step responses, the validity of the mathematical models is confirmed.

4.2.4 Thermal sensitivity model

The thermal sensitivity model of the system is developed from the frequency response of the thermal chamber test. The model thus developed contains the effect of temperature change also. Here it is considered a system of load resistance 55 ohms with bandpass filter gain 10 at a temperature of 60°C for the model. The model thus developed by using the Matlab control system toolbox is as,

$$\frac{13.66S + 2.771}{S^3 + 7.414S^2 + 12.52S + 2.771} \quad (4.1)$$

and the reference model to develop control is developed from the same system response at 25°C. It is found as,

$$\frac{0.02S + 3.4}{S^3 + 4.8S^2 + 5.9S + 3.4} \quad (4.2)$$

The bode plot for the thermal sensitive model is developed as follows,

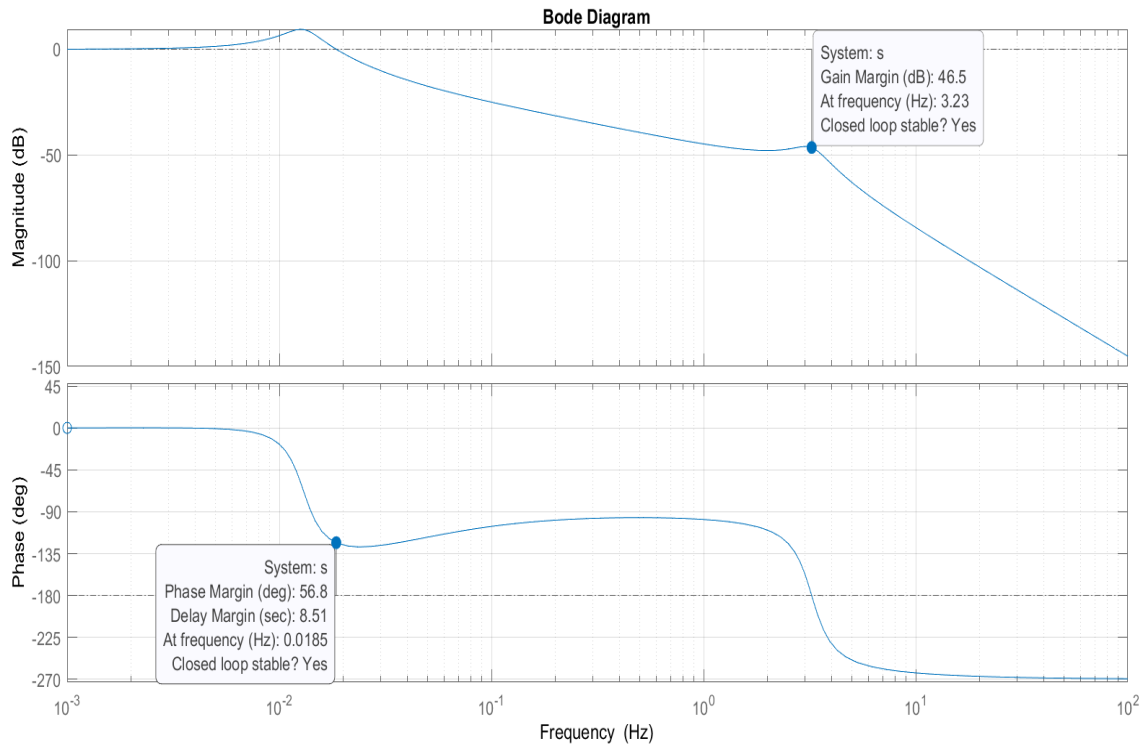


Figure 4.20: Bode plot of the thermal sensitive model developed using Matlab.

The gain margin and phase margin are positive and the system is stable, so the control can be implemented.

4.2.5 Outcomes of model reference adaptive control

Step responses of plant and reference model without adaptive control

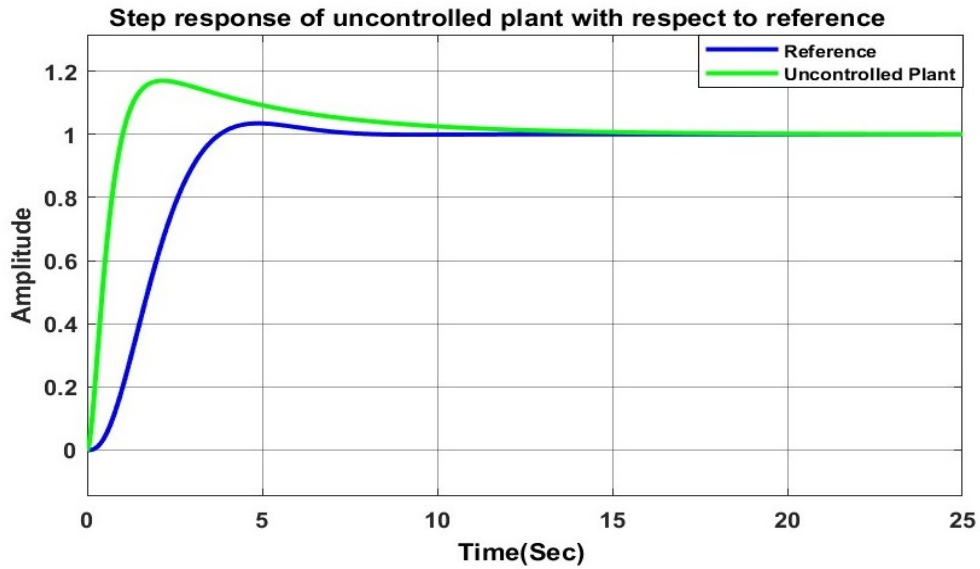


Figure 4.21: Step response of uncontrolled plant compared with the response of reference model.

The plot illustrates that the plant response, in the absence of any corrective measures for thermal effects, exhibits a significant overshoot and settling time that surpasses the desired reference model. In order to align with the reference model, it is imperative to introduce a corrective mechanism that effectively reduces the variations in overshoot and settling time.

Step responses of plant and reference model with the addition of model reference adaptive control

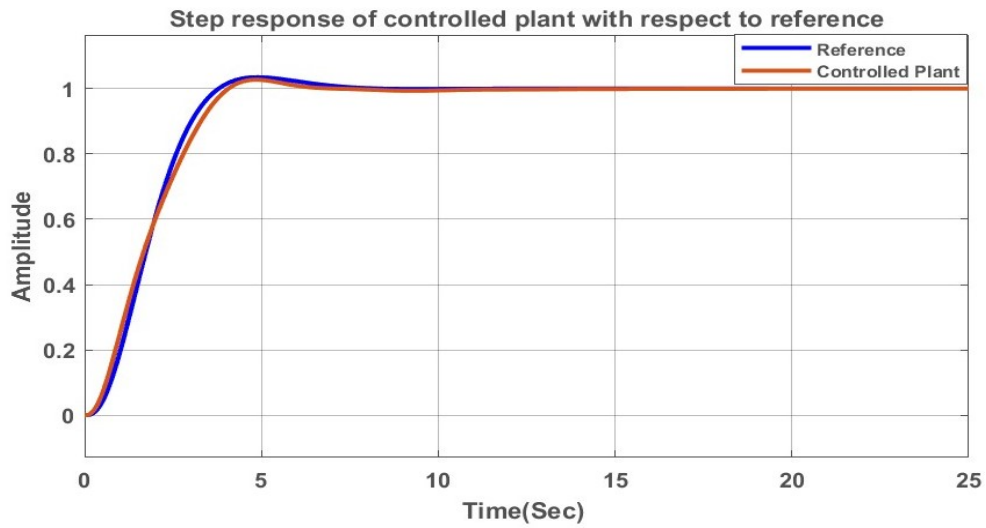


Figure 4.22: Step response of controlled plant compared with the response of reference model.

Upon the incorporation of adaptive PID control, the subsequent plot exhibits a significant reduction in both overshoot and settling time of the plant response, resulting the plant response in alignment with the response of the reference model.

Comparison of step responses with and without implementation of model reference adaptive control

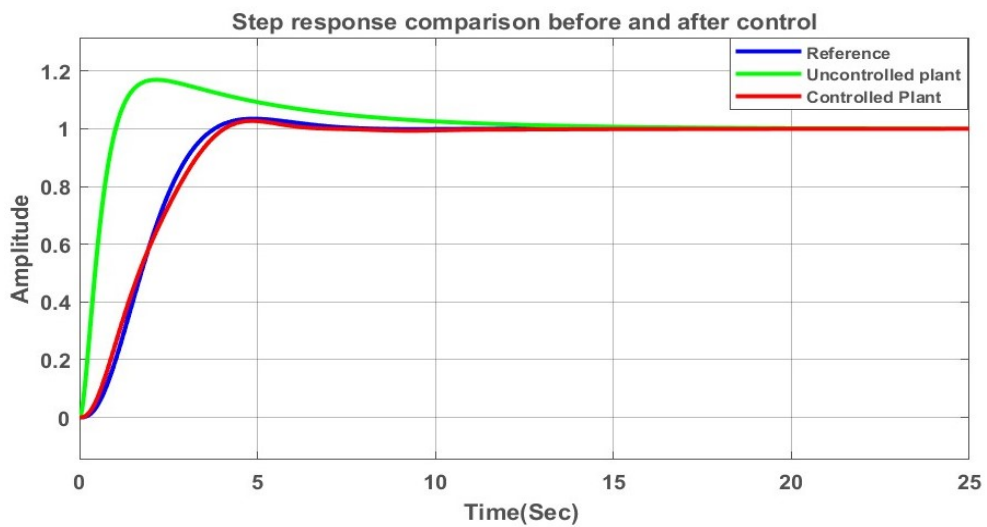


Figure 4.23: Comparison of responses before and after model reference adaptive control.

Sine response of plant and reference model without model reference adaptive control

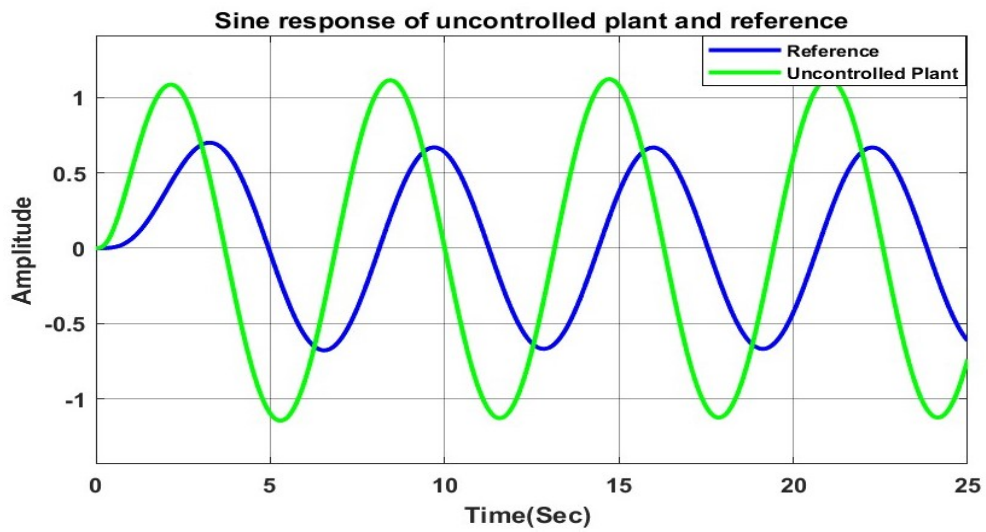


Figure 4.24: Sinusoidal response by the reference model and plant model without adaptive control.

The response of plant and reference with sine signal of magnitude $1V_{p-p}$ is as above. The plant model response is lagging behind the reference model response in an oscillatory manner.

Sine response of plant and reference model after model reference adaptive control

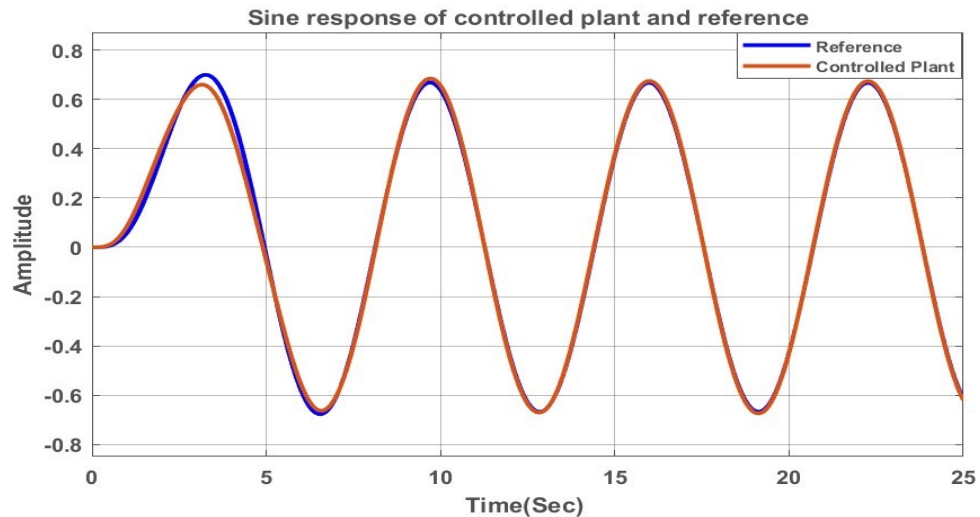


Figure 4.25: Sinusoidal response by the reference model and plant model with model reference adaptive control.

After the introduction of model reference adaptive control, the sine response of the plant adapts to the sine response of reference, thereby mitigating impact of thermal effects.

Comparison of sine responses with and without model reference adaptive control

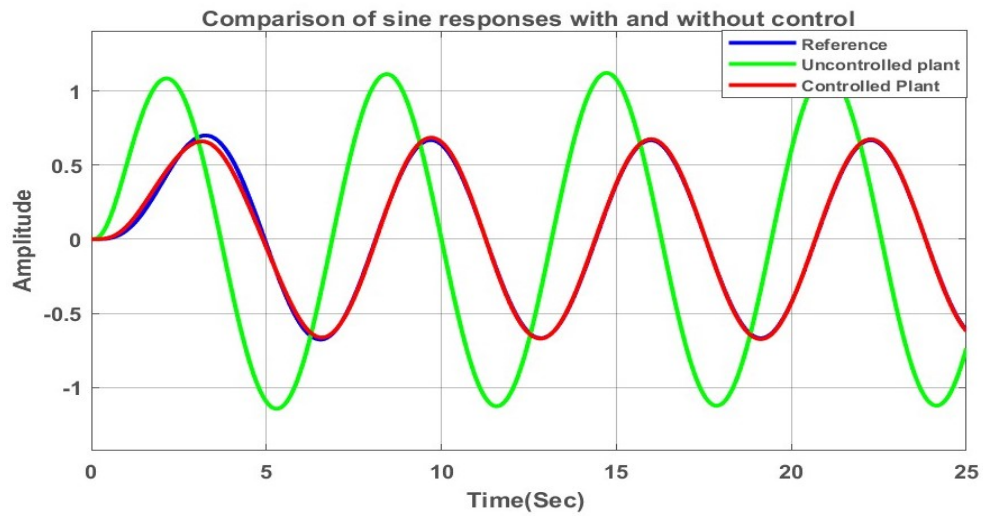


Figure 4.26: Comparison of sine responses of plant and reference with and without model reference adaptive control.

Variation of parameters θ_1 and θ_2 with respect to time

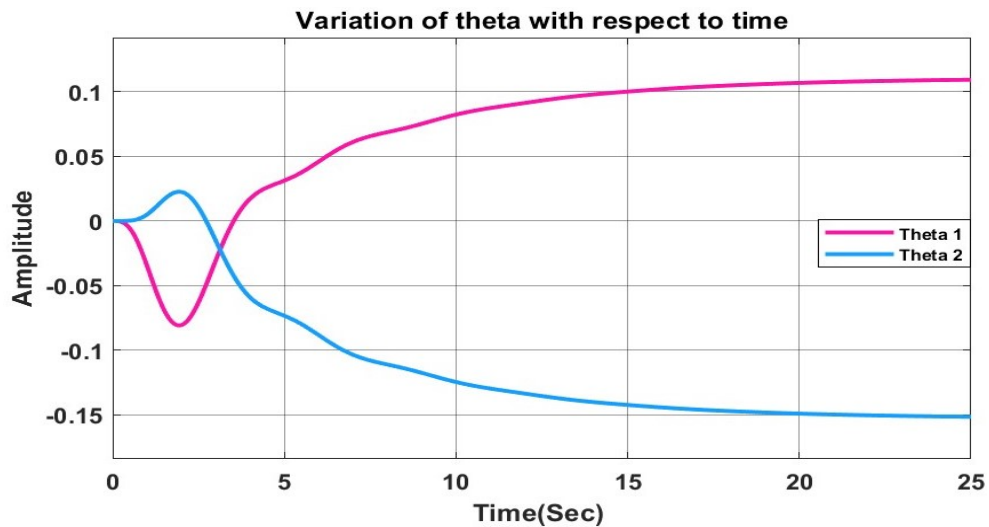


Figure 4.27: Variation happening in the values of θ_1 and θ_2 with respect to time for step input.

The parameters ' θ_1 ' and ' θ_2 ' provide the necessary correction factor for the PID controller based on the behaviour of the reference model. Analyzing the step responses reveals that the implementation of model reference adaptive control aligns the plant response with the desired reference system response. This results in a reduction in peak overshoot and settling time, bringing them in line with the response of the reference model. Examining the sinusoidal response

indicates that the plant response adapts to the reference response more rapidly. Therefore, it can be concluded that model reference adaptive control can effectively restore the thermal-sensitive model to its normal operating conditions. This control mechanism effectively mitigates the disturbances encountered at high temperatures, allowing the path length control loop to operate at its maximum potential.

4.2.6 SUMMARY

This chapter described the results of loop studies conducted to identify both the mathematical model and temperature-sensitive model. The proposed solution for controlling path length was a model reference adaptive control system, which was able to counteract external disturbances by adjusting the target plant model based on a desired model. The simulation results demonstrated the effectiveness of this solution in correcting the path length control system of the ring laser gyroscope. Without external control, there was a significant difference in the responses of the plant and reference, which was due to the effect of ambient temperature change. However, with the introduction of the external model reference adaptive control loop, the system's behaviour improved considerably and adapted to the provided model reference.

Chapter 5

CONCLUSION

5.0.1 CONCLUSIONS

Gyroscope is a device used to determine the angular position of an object. However, when external disturbances affect the measurements, the accuracy of the readings is compromised, making it challenging to predict the object's angular velocity. This becomes particularly problematic in space launch vehicles and satellites, where providing the desired altitude is crucial. To enhance the accuracy of angular velocity measurements, it is necessary to implement appropriate control strategies within the gyroscope that can withstand environmental load as well as compensation methods to mitigate the errors. In this particular project, the focus was on controlling the path length of a ring laser gyroscope to achieve a single longitudinal mode of operation. The path length control loop had certain limitations in providing effective control due to changes in ambient temperature. To address this issue, a model reference adaptive control method was proposed. To evaluate the proposed control system, Matlab simulations were conducted, utilizing mathematical models of the path length control loop developed under specific test conditions. The simulation results clearly demonstrate the effectiveness of the aforementioned control strategy in mitigating the detrimental effects of temperature changes on the path length control loop.

The approach used in this work involves linear modelling of the system to enable control implementation. However, when modelling a system experimentally, certain factors must be taken into consideration and compromises may need to be made. Linear modelling was chosen for convenience. Modelling a system using a nonlinear approach can be more complex than using

a linear approach, and may require advanced mathematical techniques and computational tools as the nonlinear equations may not have analytical solutions.

5.0.2 RECOMMENDATIONS

As a next step of this project, the hardware implementation of the MRAC system and the evaluation of the proposed scheme is recommended. If a nonlinear approach had been chosen for modelling the system, it may have been more effective as it would account for the non-linearity that might represent changes in ambient temperature. However, modelling becomes more challenging when using an experimental approach to determine the system's behaviour. As a result, numerical methods or simulation tools may be needed to solve the equations and obtain a model of the system's behaviour. Additionally, the accuracy of the resulting nonlinear model may depend on the quality and quantity of experimental data available for validation.

5.0.3 SCOPE FOR FURTHER WORK

Various control systems can be proposed in order to optimize the path length control or apply dynamic correction to existing path length control. Machine learning techniques, such as neural networks and reinforcement learning, are being employed to develop control systems that can adapt and optimize performance based on real-time data. These systems have the ability to learn from experience and improve their control strategies over time. Optimal control theory aims to find the control inputs that minimize a predefined cost function while satisfying system constraints. Recent advancements in numerical optimization algorithms and computational power have led to more efficient and practical implementation of optimal control techniques. Predictive control uses mathematical models of the system dynamics to predict future behaviour and optimize control actions accordingly. These systems consider future predictions to optimize control performance, making them suitable for applications where future states are critical. This work finds scope for improvements in the future, by understanding possible areas for development. For practical considerations, the advanced control technique selected should be at the same time, feasible for implementation in a general-purpose microcontroller.

REFERENCES

- [1] S. Dussy, D. Durrant, A. Moy, N. Perriault, and B. Celerier, “Mems gyros for space applications-overview of european activities,” in *AIAA Guidance, Navigation, and Control Conference and Exhibit*, 2005, p. 6466.
- [2] F. Aronowitz, “Fundamentals of the ring laser gyro,” *Optical gyros and their application*, vol. 339, 1999.
- [3] M. Faucheux, D. Fayoux, and J. Roland, “The ring laser gyro,” *Journal of optics*, vol. 19, no. 3, p. 101, 1988.
- [4] P. S. Begum and N. Neelima, “Development of control algorithm for ring laser gyroscope,” *International Journal of Scientific and Research Publications*, vol. 2, no. 10, pp. 1–6, 2012.
- [5] P. Pasula and R. B. Natha, “Implementation of control algorithm for ring laser gyroscope,” *International Journal of Engineering Research and Applications*, vol. 2, no. 3, pp. 850–853, 2012.
- [6] G. Chuang, W. Jian, and F. Rong, “Application of the wavelet packet analysis in the rlg strapdown ins,” in *2006 IEEE International Conference on Information Acquisition*. IEEE, 2006, pp. 926–930.
- [7] J. Ding, J. Zhang, W. Huang, and S. Chen, “Laser gyro temperature compensation using modified rbfnn,” *Sensors*, vol. 14, no. 10, pp. 18 711–18 727, 2014.
- [8] J. Cheng, J. Fang, W. Wu, and J. Li, “Temperature drift modeling and compensation of rlg based on pso tuning svm,” *Measurement*, vol. 55, pp. 246–254, 2014.

- [9] M. Wang, X. Dong, C. Qin, and J. Liu, "Adaptive h kalman filter based random drift modeling and compensation method for ring laser gyroscope," *Measurement*, vol. 167, p. 108170, 2021.
- [10] L. Ljung, "System identification toolbox," *The Matlab user's guide*, 1988.
- [11] S. Pankaj, J. S. Kumar, and R. Nema, "Comparative analysis of mit rule and lyapunov rule in model reference adaptive control scheme," *Innovative Systems Design and Engineering*, vol. 2, no. 4, pp. 154–162, 2011.
- [12] A. A. El-Samahy and M. A. Shamseldin, "Brushless dc motor tracking control using self-tuning fuzzy pid control and model reference adaptive control," *Ain Shams Engineering Journal*, vol. 9, no. 3, pp. 341–352, 2018.
- [13] A. Haber, "Introduction to Model Reference Adaptive Control with MATLAB Simulations-Fusion of Engineering, Control, Coding, Machine Learning, and Science," April 2021. [Online]. Available: <https://aleksandarhaber.com/simulation-of-model-reference-adaptive-controller-in-matlab-part-i-mit-rule-and-a-first-order-system/>
- [14] P. Jain and M. Nigam, "Design of a model reference adaptive controller using modified mit rule for a second order system," *Advance in Electronic and Electric Engineering*, vol. 3, no. 4, pp. 477–484, 2013.